This document is the Accepted Manuscript version of a Published Work that appeared in final form in *Industrial & Engineering Chemistry Research*, copyright © 2021 American Chemical Society after peer review and technical editing by the publisher. To access the final edited and published work see https://pubs.acs.org/articlesonrequest/AOR-5SGVK9EJAYA24RYDQR8J or https://doi.org/10.1021/acs.iecr.1c02938.

Polymer Blend Electrolytes for Batteries and Beyond

Michael Patrick Blatt, Daniel T. Hallinan Jr. 1,*

¹Florida A&M University-Florida State University (FAMU-FSU) College of Engineering, Tallahassee, FL, 32310, USA

Aero-propulsion, Mechatronics, and Energy Center, FAMU-FSU College of Engineering, Tallahassee, FL, 32310, USA

*Corresponding author email: dhallinan@eng.famu.fsu.edu

Keywords

Single-ion conductor, polyelectrolyte, polyanion, polysolvent, biobased, lithium metal, effective conductivity

Abstract

Polymer blend electrolytes are reemerging as an exciting class of industrially relevant electrolytes. They replace both the solvent and the salt of conventional electrolytes with polymers: termed polysolvents and polyelectrolytes, respectively. In the case of lithium batteries, the polyelectrolytes are polyanions that release lithium ions upon dissociation by polysolvents. This review defines classes of electrolytes, provides benchmarks and metrics for comparison, gives a background on polymer blends, and provides detailed review of reports on blend-based electrolytes over the past 17 years. In particular, polyether based polysolvents blended with single-ion conducting polyanions are covered, as well as biobased polysolvent blends mixed with lithium salts. A few outstanding reports meet polymer-based benchmarks but remain an order of magnitude below liquid electrolytes for lithium batteries. Therefore, an outlook is provided on

possibilities for a major breakthrough, as are recommendations for further investigation, such as the determination of mechanical properties. Currently, polymer blend electrolytes hold great potential for high energy density but low power batteries.

Introduction

Polymer blend electrolytes are reemerging as an exciting class of charged polymeric materials. The term blend is used to describe a mixture of two or more polymers. One of the main attractions of blends is the ability to formulate different compositions of synergistic macromolecular chemistries without the need for a separate polymerization, as is required for copolymers. Applications in which polymer blend electrolytes could have an impact include actuators/artificial muscles, batteries, biomedicine, desalination, and fuel cells. After a background introduction to solid-state batteries and polymer blends, this review will focus on polymer blend electrolytes for solid-state batteries. It will define nomenclature and metrics for comparing their performance and then describe recent developments in polymer blend electrolytes over the past 17 years.

Solid-State Battery Background

Motivation

As alternative energies are adopted, the need for safe, inexpensive, and energy-dense storage is of increasing importance. Since the pioneering research of Goodenough, Whittingham, and Yoshino, the lithium-ion battery has remained the preeminent battery type in portable electronics and is a leading contender for use in electric vehicles.¹ While the lithium-ion battery is a remarkable technology, recent recalls and concerns about crash integrity in electric vehicles have

motivated increased interest in alternative battery technologies to improve both safety and energy density.^{2,3} Currently, lithium-ion battery electrolytes are composed of lithium salts dissolved in organic solvents as exemplified by lithium hexafluorophosphate (LiPF₆) in organic carbonates such as diethyl carbonate (DC) and ethylene carbonate (EC).⁴ The reactive/flammable nature of these electrolytes has led to concerns about their use in transportation and personal electronics. In particular, the potential for thermal runaway, unwanted side reactions, and mechanical failure of the separator are some of the greatest concerns.^{5,6} This review will focus on a potential answer to this issue: polymer blend electrolytes.

Progress in battery technology is measured by increases in energy density and power density that can be conveniently presented in a Ragone plot,⁷ as well as cost decline. Energy density is reaching a natural plateau.⁸ Further advancement will require going beyond lithium-ion batteries by using higher specific energy electrode combinations that use conversion rather than intercalation reactions, such as lithium metal negative electrodes with sulfur or oxygen positive electrodes.⁹ Lithium's low molar mass of 6.94 g/mol give it a remarkable theoretical specific capacity of 3862 mAh/g, ten times that of graphite, and its low potential of -3.04 V versus the standard hydrogen electrode result in an exceptional specific energy as well.^{10, 11} However, lithium metal is incompatible with conventional liquid electrolytes due to rapid chemical decomposition and dendrite formation.^{4, 12} Polymer electrolytes are a promising means to combat chemical decomposition due to their electrochemical stability with alkali metals such as lithium and ability to be incorporated into mechanically strong composites that can resist dendrites.¹³ Despite the potential for higher specific energy made possible by polymer electrolytes, much slower transport of lithium ions results in a significant reduction of specific power. In short,

polymer-based electrolytes enable the construction of low power, high energy density batteries by enabling the use of otherwise excluded electrode materials.

Importance of Single-ion Conduction

The study of polymer-based electrolytes began with poly(ethylene oxide) (PEO), whose chemical structure is shown in Figure 1. Fenton, Parker, and Wright measured the conductivity of PEO when mixed with alkali salts, with conductivities near 10⁻² S/cm when the melting point of the polymer was exceeded. ^{14, 15} Interaction between ether oxygen and alkali cations enables dissociation of alkali metal salts, while the low glass transition temperature of PEO, –59 °C, enables ion transport via segmental motion. ^{16, 17} From this early discovery, research into polyether based electrolytes has become widespread in the literature. However, a persistent issue has been the relatively low steady state current densities of polymer electrolytes when compared to conventional liquid electrolytes and the formation of dendrites.

$$\left\{ \right\}_{n}^{\circ}$$

Figure 1. Poly(ethylene oxide).

In the battery field, the polymer blend electrolyte movement was preceded by earlier works to form single-ion conducting copolymers based on PEO and charge containing monomer units, typically derived from lithium salts. An early series of PEO-perfluorosulfonate copolymers was generated by Armand and coworkers in 1995. Lithium salts were functionalized using epoxy or alkene groups. The monomers were lithium N,N-diallyl-1-amido-tetrafluoro-ethanesulfonate (DaaR_FSO₃Li), allyloxy-2-tetrafluoroethylsulfonyl fluoride (AlR_fSO₃Li), and glycydoxy-2-tetrafluoroethanesulfonyl fluoride (GlyR_FSO₃Li). Each of these monomers was then

copolymerized with PEO, to achieve O:Li ratios of 8:1 and 16:1. The most effective of these copolymers was a 16:1 PEO to AlR_fSO₃Li ratio with conductivities on the order of 10⁻⁴ S/cm.

This impressive ionic conductivity in a single-ion conducting copolymer has led to much research on copolymers of polysolvents and polyanions, largely preceding studies of polymer blend electrolytes for lithium batteries. In these copolymers the two components are combined covalently and the composition is fixed at the time of synthesis. The reader is referred to comprehensive recent reviews that cover this other promising class of polymer electrolytes for more detail. 19-22 In particular, the review by Strauss et al. and the exhaustive review by Zhang et al. cover important advancements in single-ion conducting copolymers since the seminal work of Armand's group in the 1990's. 19, 20 Due primarily to polysolvent design that suppresses crystallinity, copolymers have demonstrated superior performance to that of blends, especially at room temperature.²³ Despite this, interest in blend electrolytes is growing, for the most part due to the ability to determine composition after synthesis, but perhaps also due to the relatively limited attention this approach has received as well as the possibility for independent design of polysolvent and polyanion. A potential pitfall of blend electrolytes is macrophase separation. Unlike copolymer electrolytes in which it is sometimes possible to retain component properties in the microphase separated state, phase separation of blends occurs on macroscopic scales that are more likely to detrimentally impact material properties. This is true for polymer blend electrolytes (the focus of this review) as well as composite electrolytes of polymers and inorganic particles, another growing class of electrolytes covered in more general recent reviews on solid electrolytes. ^{20, 22} However, studies reviewed herein have demonstrated that considerable phase space is available in which polysolvents and polyanions are miscible.

In 1999, Newman, Kerr, and coworkers provided powerful support for the use of chargecontaining polyether copolymers through the simulation of the relative performance of different classes of polymer electrolytes in a contemporaneously common battery set up of Li metal polymer | LiV₆O₁₃.²⁴ This work compared the relative efficacy of the then field-leading binary polymer electrolyte, oxymethylene-linked poly(ethylene glycol) (PEMO) with lithium bis(trifluoromethyl sulfonyl) imide (LiTFSI) salt, and the leading single-ion conductor, a random copolymer containing lithium sulfonated methylpolyethylene glycol acrylate (LiPEGA). Computational models developed earlier by Fuller and Newman²⁵ were applied to simulate the cycling of these two classes of batteries. Of note were the advantages offered by the reduced concentration gradients observed in what they termed the ionomer electrolyte. After three hours of elapsed simulation time, the binary electrolyte featured a much larger concentration gradient due to relatively equal mobility of the cation and anion while much more of the charge in the ionomer membrane was carried by the cation, leading to a reduced concentration gradient. These simulations suggest that both the specific energy and the steady state current density of the ionomer (LiPEGA) electrolyte was higher than the polymer electrolyte (PEMO + LiTFSI). The specific energy and current density that could be achieved with LiPEGA was 41 Wh/kg and 0.25 mA/cm² while with PEMO values of 31 Wh/kg and 0.20 mA/cm² were possible. Thus, this paper provided a powerful argument for the use of single-ion conducting polymers to overcome the low currents of polymer electrolyte batteries.

The reduction in concentration gradients simulated by Newman and coworkers in 1999 reveals a major advantage of polyanion-based single-ion conductors that has spurred recent research. During discharge in lithium metal batteries, lithium cations participate in the reactions with the electrodes. Conversely, the anion is not involved in the electrochemical reactions. Thus,

if anion mobility can be restricted, a greater proportion of the electrochemical energy in the cell goes towards transporting the cations involved in the redox reactions that generate (or store) energy during discharging (or charging). This relative amount of charge carried by the cation versus the anion is represented via the cation transference number, t_+ .

There are two relatively straightforward methods for determining t_+ . The first, pioneered by Vincent, Bruce, and Evans, uses a cell with reversible electrodes and applies a constant voltage. 26,27 $t_{+,SS}$ is the ratio of the initial current to the steady-state current. The second calculates $t_{+,NMR}$ from self-diffusion coefficients of the cations and anions measured with pulsed field gradient nuclear magnet resonance (PFG-NMR). $^{28-30}$ Both of these techniques rely on dilute solution approximations. In other words, they break down if the electrolyte is not fully dissociated. Since we know that PEO-based electrolytes are not fully dissociated at salt concentrations relevant to batteries, an alternative approach is necessary.

A third more complicated approach developed by Newman and coworkers uses potential measurements to determine the change in concentration near each electrode after the passage of current.³¹ In order to account for nonideality, a calibration between potential and concentration must be conducted with concentration cells and logarithmic slopes calculated. In addition, the diffusion coefficient must be known. Therefore, this approach requires three separate measurements to determine t^0_+ . Its distinct advantage over the first two methods is that it holds in concentrated solution for any complex set of dissociation states. A variant of this approach was applied by Balsara and coworkers and compared to the first two methods.³² Their results indicate that ion speciation leads to much lower t^0_+ at high salt concentrations than expected based on dilute solution theory. Their result is in reasonable agreement with a fourth, more direct method for measuring t^0_+ called the Hittorf method³³ that was used by Bruce and coworkers on a similar

polymer electrolyte.³⁴ The Hittorf method determines t^{0}_{+} as the ratio of change in moles of salt near an electrode, Δn_{salt} , in response to the total applied charge, Q. The change in moles is converted to charge with Faraday's constant, F. The Hittorf method is appropriate for semi-dilute and concentrated electrolytes, and the primary difficulty is avoiding mixing,³⁵ which is not a problem in polymer electrolytes. In the original work the cell was disassembled and sectioned and the following expression used to calculate transference number.³⁴

$$1 - t_{+}^{0} = \frac{\Delta n_{salt} F}{Q} = \frac{\text{Charge carried by anion}}{\text{Total charge transferred}}$$
 (1)

The only significant limitation of this method is that sufficiently small Q must be applied to prevent the concentration gradient from extending fully across the electrolyte, whereby transport due to diffusion would introduce error into the measurement. An interesting recent method, that relies on time-resolved X-ray scattering and simulations, has found a more or less constant t_+^0 . Based on mediocre agreement among different techniques, a simple but accurate method to reliably determine this important parameter would be a significant contribution to the field.

As implied by Equation 1, during discharging or charging of a battery a salt concentration gradient develops that is negatively correlated with the transference number of the reactive ion. This concentration gradient causes a concentration overpotential. In other words, it increases the difference between charging voltage and discharging voltage. The energy to charge or discharge the cell is the product of the charged passed and the voltage. The energy efficiency then is

$$\eta = \frac{\int_{discharge} Vi \, dt}{\int_{charge} Vi \, dt}.$$
 (2)

Thus, the smaller the difference between charge and discharge voltage the greater the energy efficiency. A perfect single-ion conductor will not have a concentration gradient and will not have energy efficiency losses due to concentration overpotential. 37-39 Moreover, lithium dendrite formation is correlated with concentration gradients, 40-42 and a lack of concentration gradient in single-ion conductors has been reported to retard lithium dendrite formation. 43, 44 These benefits drive efforts to develop single-ion conductors. The additional motivation to avoid flammable volatile components, such as organic solvents, but the need for some solvating species has recently led the field to polymer blend electrolytes.

Early Charged Polymer Blends

About ten years after the discovery that alkali metal salts dissolve in PEO, the Eisenberg group published a seminal study demonstrating that ion-dipole interactions lead to blend miscibility. In this study, a styrene-lithium methacrylate copolymer was blended with PEO or poly(propylene oxide). Interestingly, their group demonstrated that numerous polar polymers are miscible with polystyrene ionomers. In the early 1990's, Tsuchida and coworkers investigated blends of polyanions with alkali metal counterions (including Li⁺) with oligo(oxyethylene). Their studies were the earliest demonstration that, in addition to segmental motion, the strength of the ion-dipole interaction affects ionic conductivity. This observation has since been verified with conductivity and rheology measurements.

Since the early work on random copolymers and ionomer blends, focus has shifted to block copolymers containing both solvating and ionic components. Notable work has been done by Balsara, Park, and their respective collaborators to study and manipulate the morphologies of single ion conducting block copolymer electrolytes to enhance transport properties. ⁴⁹⁻⁵⁵ In recent years, the use of polymer blends has become more common. This movement is a consequence of

the relative ease of forming blends of differing composition and the similarity between miscible block copolymers and miscible blends. This review will focus primarily on the methodology and findings relating to polymer blend electrolytes. Figure 2 shows the growth of the field by displaying the number of yearly publications and citations containing the key words "Polymer Blend Electrolytes" in the past 30 years. For context, "Polymer Blend Electrolytes" have increased from roughly 5% to 8.5% of all publications concerning "Polymer Electrolytes" during the period of 2000-2020. As Figure 2 shows, interest in polymer blend electrolytes has persistently increased in this young subfield over the last 20 years.

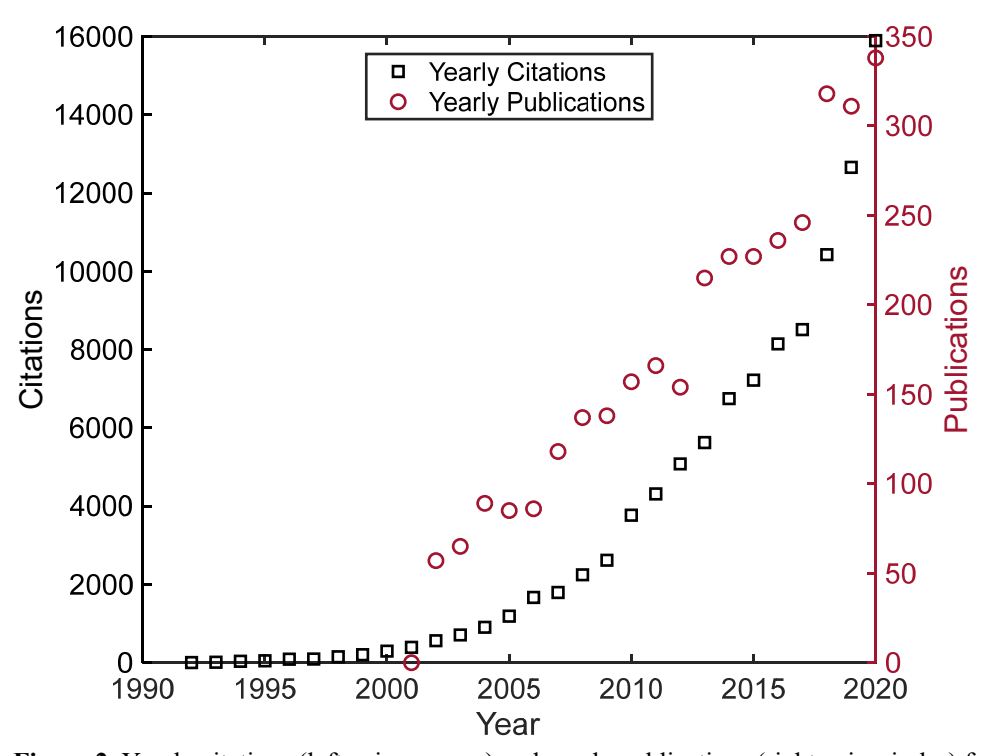


Figure 2. Yearly citations (left axis, squares) and yearly publications (right axis, circles) for "Polymer Blend Electrolytes" as tracked by *Web of Science*. ⁵⁶

Polymer Blend Background

Polymer Blend Thermodynamics

Neutral polymer blends have been a classic area of soft matter research.⁵⁷ Fundamental understanding of how entropy and enthalpy (i.e. specific interactions) affect miscibility of polymer blends has, for the most part, been developed in the context of Flory-Huggins Theory. This statistical thermodynamic approach adapted lattice theory for polymers by accounting for the much larger size of polymer molecules. 58 In contrast to small molecules, in which entropy can significantly promote mixing, the contribution of entropy to mixing in polymer blends is much smaller. As shown in Equation 3, this is due to the penalty of long chains, embodied in the degree of polymerization, N_i , appearing in the denominator of the first two terms on the righthand side (RHS). Thus, specific interactions, embodied by the Flory-Huggins interaction parameter (χ) , play an important role in determining blend miscibility. The energy change upon mixing can be written in terms of the Helmholtz free energy (for a constant volume system)⁵⁹ or in terms of the Gibbs free energy (for a constant pressure system).⁵⁸ The latter tends to be more representative of experimental conditions. Two equivalent expressions for the Gibbs free energy change upon mixing per lattice site, $\Delta \bar{G}_{mix}$, are presented in Equations 3 and 4.60 The Gibbs free energy of mixing per unit volume, ΔG_{mix} , is simply related to $\Delta \bar{G}_{mix} = \Delta G_{mix} V_{ref}$ via the volume of a lattice site, V_{ref} , which can be arbitrarily chosen.

$$\frac{\Delta \bar{G}_{mix}}{kT} = \frac{\phi_A}{N_A} ln \phi_A + \frac{\phi_B}{N_B} ln \phi_B + \phi_A \phi_B \chi \qquad (3)$$

$$\frac{\Delta \bar{G}_{mix}}{RT} = V_{ref} \left[\frac{\rho_A \phi_A}{M_A} ln \phi_A + \frac{\rho_B \phi_B}{M_B} ln \phi_B \right] + \phi_A \phi_B \chi / A_v$$
 (4)

Equation 3 is preferable in the sense that it is unitless, whereas Equation 4 is convenient in that measurable quantities of density, ρ_i , and molecular weight, M_i , are used. The gas constant is related to the Boltzmann constant via Avogadro's number, $R = kA_v$. Furthermore, the degree of

polymerization (defined as the number of reference volumes comprising each chain) is related to the physical properties of component i, $1/N_iA_v = V_{ref}\rho_i/M_i$.

If $\Delta \bar{G}_{mix}$ is negative the blend is miscible, and if its second derivative with respect to volume fraction is positive then it is a stable state.⁶¹ Equations 3 and 4 are written in terms of volume fraction, with $\phi_A + \phi_B = 1$ for a binary blend of A and B. The simplicity of Flory-Huggins Theory is the reason it continues to be used even for systems such as polymer blend electrolytes, for which it was not developed. The third term in Equation 3 fundamentally accounts only for excluded volume interactions. However, an effective interaction parameter (χ_{eff}) is frequently used (especially by experimentalists) as a fitting parameter to account for all thermodynamic interactions.⁶² Various empirical expression have been developed to account for the temperature and concentration dependence of χ_{eff} . The most common expression is $\chi_{eff} = A + \frac{B}{T}$, and values for parameters A and B have been tabulated for a wide range of neutral polymer blends.⁶⁰

While χ_{eff} is a simple, convenient metric to compare behavior of polymer blends, work from the Olvera de la Cruz group has demonstrated that rich phase behavior is possible in charge containing systems due to the complex dependence of χ_{eff} on composition and strength of electrostatic interactions.⁶³ Figure 3 demonstrates how ion interactions can affect the phase diagram of polymer blend electrolytes. For simplicity, only spinodal curves are shown. The neutral case is for a symmetric blend of PEO and PS (i.e. $N_{PEO} = N_{PS} = 40$). The degree of polymerization is the same in the cases where component A is charged, but ion interactions clearly result in an asymmetrical phase diagram. It is interesting to note that weak ion interaction promotes mixing at all compositions, despite the fact that the neutral contributions to the interaction parameter are unchanged. In other words, the effect shown is purely due to

correlation between, for example, polyanions and counter cations. It is remarkable that, without introducing any explicit ion-dipole interactions, addition of charge to a polymer can promote blend miscibility, although the dielectric constant of the medium does play a role in the mean-field approach used by Sing and Olvera de la Cruz.⁶³ In retrospect, it is surprising that the knowledge from last century: that ionomers can promote blend miscibility⁶⁴ did not gain traction more rapidly in the polymer electrolyte field. This may be due in part to the complexity that charge interactions can bring to the blend phase diagram. As the strong-interaction case shows, when ions are strongly correlated a miscibility gap is present for small amounts of the charged polymer. The miscibility gap gets larger with increasing ion interaction strength. Within this gap, the critical interaction parameter for spinodal decomposition is negative, such that a system with a negative γ could phase separate.

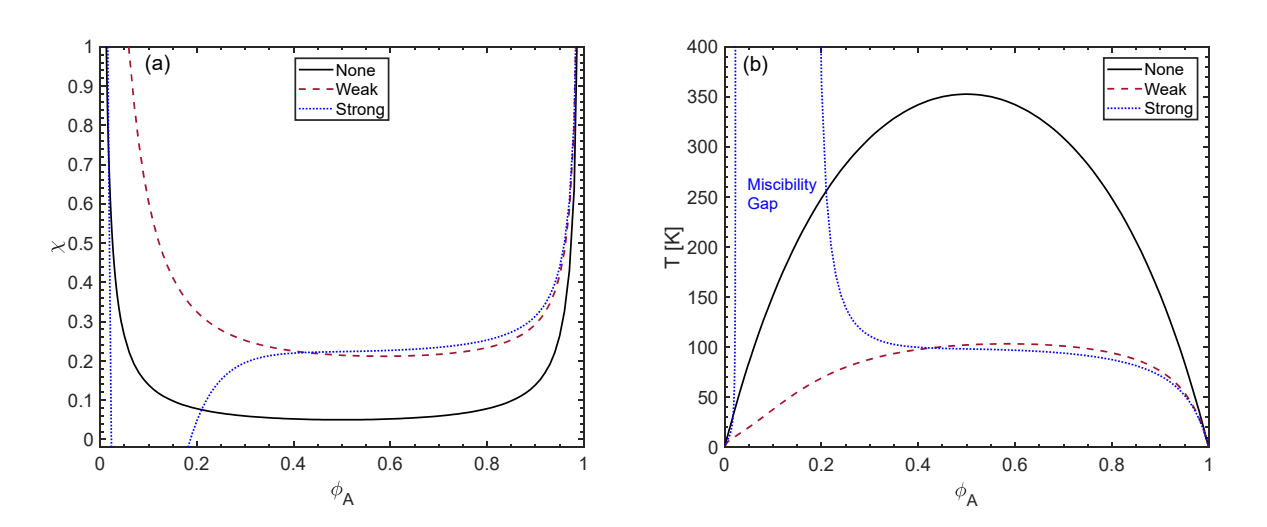


Figure 3. Spinodal phase diagram of blends demonstrating the effect of ion correlation. The ion interaction strength is denoted in each legend. The neutral case (no ion interaction strength) is for PEO/PS with N=40. (a) The critical interaction parameter for spinodal decomposition in the neutral case was calculated $\chi=\frac{1}{2N\phi_A\phi_B}$. ⁶⁰ The contribution from charge interaction, α , was added to the neutral χ value. Values of α were estimated from Sing and Olvera de la Cruz. ⁶³ (b) The spinodal curve was calculated $T=\frac{B}{\chi-A}$, where $A=-1.72\times10^{-2}$ and B=23.7. ⁶⁰

There are four primary methods by which polymer blends have been prepared: 1) Solvent casting, 2) Precipitation from a solvent, 3) Freeze drying a solution, and 4) Melt mixing. For solvent casting, the two polymers are dissolved in a co-solvent, spread on a level surface, and the solvent evaporated to yield a film or membrane. Solvent casting can trap miscible blends in an immiscible region of the ternary (polymer-polymer-solvent) phase diagram. On the other hand, it can kinetically trap immiscible blends in a homogeneous mixture due to the compatibilizing effect of the solvent. Finally, solvent casting can promote crystallization and result in apparent immiscibility. 65 Despite these drawbacks, it is a convenient method for generating membranes; it is compatible with small quantities; and is therefore widely used in research studies, especially those concerning polymer blend electrolytes. Precipitation is an alternative method that avoids most of the drawbacks of solvent casting. With this method, the solution of polymers in cosolvent is poured into a poor solvent to rapidly precipitate the blend. A common method for thoroughly removing solvent from a polymer solution is freeze drying. In this method, the solution is frozen, placed under vacuum, and the solvent molecules sublimed (rather than evaporated). This method results in a foam or powder, depending on the initial polymer concentration of the solution. The porous pathways for solvent to escape lead to more complete removal of solvent, but the process is slow. Unlike water, whose heat of sublimation is sufficient to keep the frozen solution from melting, organic solvents require a freeze dryer that actively cools the solution, which requires additional energy. The fourth method, melt mixing, is often conducted in an extruder. This method avoids any concerns of residual solvent in the blend, a concern in batteries if the solvent reacts with the electrodes. Residual solvent is a particular concern due to strong coordination that has been observed between polar solvents and ions⁶⁶/polyelectrolytes⁶⁷ that makes complete removal of the solvent difficult or impossible.

However, the thermal and mechanical stresses of melt mixing can cause degradation of certain polymers.⁶¹

Polymer Blend Characterization

Due to the importance of blend miscibility on blend properties, several techniques have been developed to determine if a blend is miscible. The simplest approach is to use visual inspection or optical microscopy to identify macrophase separation. If the pure components are clear, then a miscible blend will be transparent. Macrophase separation of the blend into domains of different refractive indices on a size scale commensurate with visible light wavelengths will scatter light and make the blend appear cloudy. This requires the pure components to have a refractive index difference greater than 0.01.⁶¹ The same approach can be used in a quantitative manner with light scattering. Using a laser-based set-up and measuring changes in scattering intensity, it is possible to determine the compositions and temperatures at which phase separation occurs. The aforementioned techniques cannot be applied when one of the pure components is opaque or translucent. This is the case for semicrystalline polymers, such as PEO, and for many charged polymers, such as sulfonated polystyrene.⁶⁸ Thus, optical/light scattering based approaches are not possible for many of the polymer blend electrolytes discussed in this review.

In the case when pure components are semicrystalline, melting point depression can be used to determine miscibility. Melting point depression is a colligative property: the amount of depression depends on the moles of noncrystallizable component in the homogeneous melt (from which the crystals are forming). As shown by Flory for small-molecule diluent⁶⁹ and separately by Nishi and Wang for polymeric diluent⁷⁰ (derived using thermodynamic expressions of Scott and Magat⁷¹), it can be used to find χ . Specifically, the melting temperature of the blend, T_m , in

reference to the melting temperature of the pure component, T_m^0 , in terms of volume fraction of diluent, ϕ_1 , is as follows.

$$\frac{1}{T_m} - \frac{1}{T_m^0} = \frac{R\hat{V}_{2u}}{\Delta \hat{H}_m^0 \hat{V}_{1u}} \left[\frac{\phi_1}{N_1} - \chi \phi_1^2 \right]$$
 (5)

If the molar enthalpy of melting of the semicrystalline component $(\Delta \hat{H}_m^0)$ and the molar volumes of the repeat units of the components (\hat{V}_{iu}) are known, then χ can be found. Moreover, for sufficiently high molecular weight of the amorphous polymer acting as diluent in the blend, $N_1 \to \infty$, and the first term on the RHS of Equation 5 goes to zero. The derivation of this expression assumes volume additivity, which may be an acceptable assumption even for ion containing systems. 72, 73 It also assumes that the interaction energy between components is the harmonic average of their self-interaction energies, which is a poor assumption if electrostatic interactions are present. Nonetheless, it has been used recently to determine an effective interaction parameter in a polymer blend electrolyte. 74

Care should be taken to verify miscibility with an independent technique, because there are examples of immiscible blends that exhibit T_m depression, such as isotactic polystyrene/poly(methyl methacrylate) (iPS/PMMA)⁶⁵ and miscible blends that do not show clear T_m depression, such as PEO/PMMA.⁷⁵ Technically, the equilibrium melting temperature should be used.⁷⁶ The equilibrium melting temperature is most commonly found with the Hoffman-Weeks approach, which relies on several assumptions. A more rigorous method is the Gibbs-Thomson approach.⁷⁶ Nishi and Wang found little dependence of heating rate on T_m in poly(vinylidene fluoride) (PVDF)/PMMA blends.⁷⁰ This suggests that using equilibrium melting temperature is not essential. As shown in Figure 4, quenched samples of PEO/PMMA gave T_m depression results that agree with the general consensus that PEO/PMMA are fully miscible,

whereas isothermally crystallized blends indicated otherwise.⁷⁷ Barring a more sophisticated approach, such as neutron scattering described below that requires much more complex analysis, melting point depression is an accessible method for estimating effective interaction energy in polymer blend electrolytes.

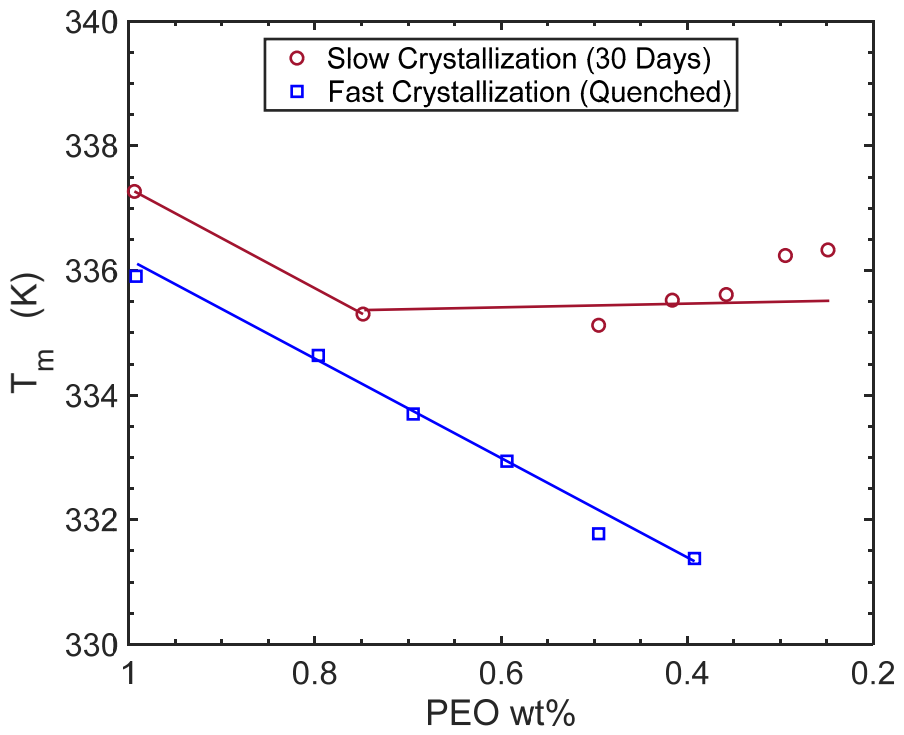


Figure 4. Melting temperature of PEO/PMMA blends as a function of PEO wt%. The blends were solution cast and either crystallized at room temperature for 30 days (circles) or quenched from 120 °C (squares). Reproduced from Li and Hsu.⁷⁷

Another indication of blend miscibility is glass transition temperature, T_g . It is generally considered that a homogeneous melt will show a single T_g , whereas a phase-separated system will show two T_g 's. It was discovered in the mid-2000s that this is not always true. This unexpected behavior is most noticeable in blends with large T_g difference between those of the pure components, like PEO/PMMA. It is due to self-concentration. That is, chain connectivity

causes the concentration within a Kuhn monomer volume to be enriched in the polymer's own segments. This is captured by the Lodge-McLeish (LM) Model.

$$\phi_{eff} \equiv \phi_{self} + (1 - \phi_{self}) \langle \phi \rangle$$
 (6)

where the effective volume fraction of a component, ϕ_{eff} , is a function of its macroscopically averaged volume fraction, $\langle \phi \rangle$, and an enrichment factor, ϕ_{self} , that can be used as a fitting parameter. The local effective concentration for each component can then be used in an appropriate model, such as the Fox equation, 80 to find the T_g of each component.

$$\frac{1}{T_{g,i}(\langle \phi \rangle)} = \frac{\phi_{eff}}{T_{g,i}} + \frac{\left(1 - \phi_{eff}\right)}{T_{g,j}} \tag{7}$$

Although there is a $T_{g,i}$ for each component i, they do change with composition. Thus, the composition-dependence of T_g can still be used to infer miscibility (supported by other techniques).

There are numerous methods for measuring T_g ; the most common include differential scanning calorimetry (DSC), dynamic mechanical analysis (DMA), dielectric spectroscopy, and dilatometry.⁶¹ DSC measures heat flow (to/from the sample), q, that is due to heat capacity of the material, C_p , and any kinetic processes such as phase changes, f.

$$q = C_p \frac{dT}{dt} + f(T, t)$$
 (8)

Heat capacity changes at T_g , causing an inflection point in the heat flow curve. A round robin test on PS with 10 different instruments used a standard heating/cooling rate of 20 K/min and took the T_g as the midpoint of the inflection on the second heating run. This study by Rieger

discusses the effects of cooling rate, analysis method, and sample mass on measured T_q . 81 In order to remove user bias, it has been recommended to find T_g by taking the maximum of the smoothed temperature derivative of heat flow.⁷⁹ DMA takes advantage of the large change in mechanical properties on transitioning from a glass to a rubber by probing the sample with small-amplitude oscillations (typically either in shear or in tension). Small-amplitude means that the sample's mechanical properties are probed without causing irreversible deformation. In another study by Rieger using 83 different polymer systems, it was shown that T_g from DMA agrees well with that from DSC when a frequency of 1 Hz is used and the maximum of the shear (or tensile) storage modulus, G'' (or E''), is used rather than $\delta = G''/G'$. 82 Dielectric spectroscopy is a sensitive technique that measures dipole reorientation and charge displacement in response to an oscillating electric field. It has been used to measure polymer relaxations across an extremely wide range of time scales (18 orders of magnitude), including T_q .⁸³ Finally, dilatometry measures volume change as a function of temperature (and pressure). Dilatometry can be used because the thermal expansion coefficient changes at T_g . A fantastic compilation of dilatometry measurements on many different polymers is available in the book by Zoller and Walsh.84

In addition to the numerous methods for measuring T_g , numerous models have been developed to account for the dependence of T_g on the composition of miscible polymer blends. The simplest is the Fox equation mentioned above. Like the Fox equation, the Gordon-Taylor equation assumes volume additivity, but it accounts for different densities of the components. For equal densities, it simplifies to the rule of mixtures. The Kwei equation (derived by Kanig) contains a quadratic concentration correction that accounts for specific interactions (deviations from additivity). In a nice review of the T_g 's of polymer blends, Schneider presents all these

models and a graphical method for determining which model to use. Plotted in the manner of Figure 5, the Gordon-Taylor equation yields a flat line with a value of one (e.g. PS/PPO); the Kwei equation yields a straight line with a slope (e.g. PVME/PS and PVDF/PMMA); and a third power equation can account for deviations from linearity (e.g. PS/P α MS and PDNBM/PHMCM). Acronyms are defined in the caption of Figure 5. Relevant to polymer blend electrolytes, hydrogen bonding and charge transfer can cause positive deviations from linearity, as exemplified by PMMA/PVDF. The corrected weight fraction of the higher T_g component, w_{2c} , is used in Figure 5. This representation can be understood by beginning with the commonly used Gordon-Taylor equation.

$$T_g = \frac{w_1 T_{g1} + K w_2 T_{g2}}{w_1 + K w_2} \tag{9}$$

Subtracting T_{g1} from both sides and rearranging yields

$$\frac{T_g - T_{g1}}{T_{g2} - T_{g1}} = \frac{Kw_2}{(w_1 + Kw_2)} = w_{2c}$$
 (10)

K is a ratio of the following values for each component: T_g , density, and difference of thermal expansion coefficients of glassy and rubbery states. Due to limited data, K is often treated as a fitting parameter. Schneider suggests a generalized expression that is third-order in weight fraction.

$$\frac{T_g - T_{g1}}{T_{g2} - T_{g1}} = (1 + K_1)w_{2c} - (K_1 + K_2)w_{2c}^2 + K_2w_{2c}^3$$
 (11)

For the Gordon-Taylor equation, $K_1 = K_2 = 0$, and for the Kwei equation $K_2 = 0$. The reader is referred to Schneider's review for detailed discussion of the connection of these parameters to interaction energies and other physical constants.⁸⁵

In the polymer blend electrolyte literature, application of these models to T_g data is rare. This is due, primarily, to the T_g being determined at an insufficient number of different compositions. Of the studies discussed in this review, few contain DSC thermograms for 3 unique compositions, preventing comparison of the relative efficacy of each T_g model. One exception was Müller's group, who did analyze T_g of a blend of PEO and poly(lithium 1-[3-(methacryloyloxy) propylsulfonyl]-1-(trifluoromethanesulfonyl)imide) (PLiMTFSI) using the Gordon-Taylor equation.⁷⁴ As with any application of a model to experimental data, the fewest number of fitting parameters that accurately represents the data should be used. It seems that despite polar and ionic interactions present in the blends, composition-dependent effects were not significant, such that the data was well fit by the Gordon-Taylor equation. However, an upturn in the data is apparent in Figure 5 at low PLiMTFSI content, where the miscibility gap occurs for systems with strongly correlated ions and where PEO crystallization is expected to be most significant. It was reported that values of K increased with increasing polyanion molecular weight (at fixed PEO molecular weight), which is somewhat surprising based on the proportionality of K to component densities and thermal expansion coefficients. The data in Figure 5 is for 100 kg/mol PEO and 50 kg/mol PLiMTFSI. The upturn was more significant for 5 kg/mol PLiMTFSI (not shown) and nonexistent for >2,000 kg/mol PLiMTFSI (also not shown), which exhibited values less than 1. Thus, molecular-weight-dependent effects appear to be subsumed into the empirical value of K. Although the Gordon-Taylor equation appears to fit the data of this polymer blend electrolyte rather well on a simple plot of T_g versus weight fraction, the representation suggested by Schneider makes it clear that other effects, such as crystallinity and ionic interactions, cause a divergence from the model for blends dilute in the electrolyte. Due to the significant impact of polymer segmental mobility on electrolyte conductivity,

complete characterization of blend T_g in a larger number of polymer blend electrolyte studies would enable the field to develop the knowledge needed for predictive material design. Future work should focus on determining the blend T_g at all compositions investigated, and modeling should begin with the Gordon-Taylor equation.

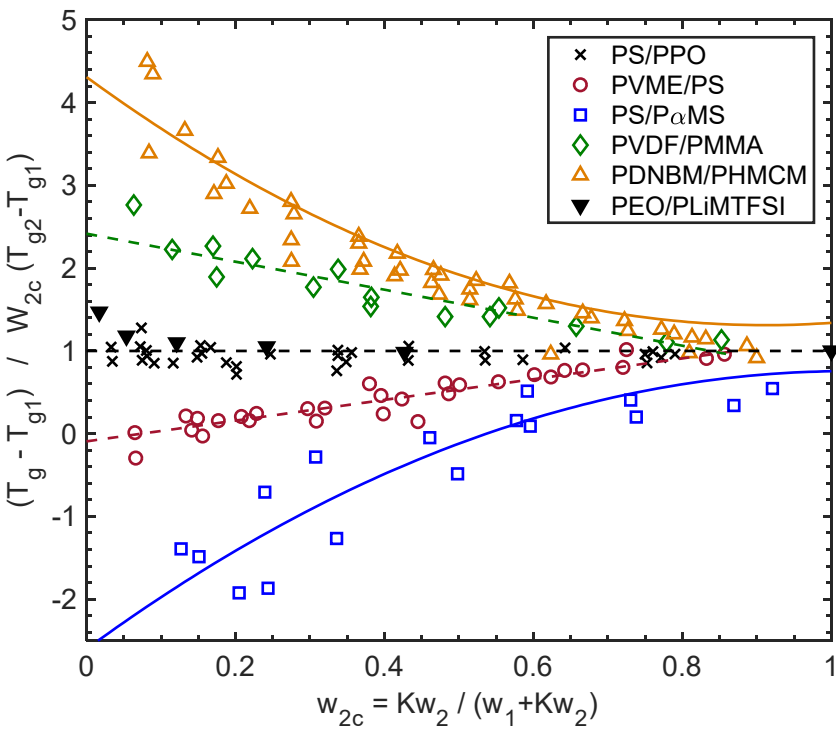


Figure 5. Plot of normalized blend T_g versus corrected weight fraction of the higher T_g component, w_{2c} , for noted blends. Normalized T_g is divided by w_{2c} to aid in model selection. First five data sets (in order of legend) reproduced from Schneider. Final data set calculated from data reported in Olmedo-Martínez et al. PPO = poly(2,6-dimethylphenylene oxide), PVME = poly(vinyl methyl ether), PαMS = poly(α-methylstyrene), PDNBM = poly(β-hydroxyethyl-3,5-dinitrobenzoyl methacrylate), and PHMCM = poly(N-ethylcarbazol-3-yl-methyl methacrylate).

The most reliable method to determine phase miscibility of polymers is to use small-angle neutron scattering (SANS) modeled with the Random Phase Approximation (RPA). 86-88 SANS of a homogeneous melt will yield a predictable scattering pattern that can be fit with RPA to find the interaction parameter as a function of temperature, $\chi(T)$. This approach usually requires that

one of the polymers be deuterated, which adds great expense unless one relies on a national user facility to support material synthesis. It should be noted that although deuterated compounds are commonly considered chemically identical to their non-deuterated counterparts, isotope effects (though small) have been seen to cause phase separation in polymer blends with small χ .⁸⁹ Neutrons are generated by nuclear reactors, which severely limits accessibility. So, while it is the gold standard, it can only be applied to select systems with a compelling motivation to do so.

Definitions and Nomenclature

Before discussing the specific polymer blend electrolyte systems in recent literature, a fundamental understanding of the key components of electrolytes is important. With the exception of molten salt electrolytes, an electrolyte is composed of two principal components: a salt and a solvent. In the presence of solvent (or above its melting temperature), the salt dissociates into positive ions (cations) and negative ions (anions).^{4,90} The solvent enables dissociation of the salt into its constituent ions and facilitates transport of the ions via diffusion and migration. Diffusion describes transport driven by concentration gradients while migration describes the movement of ions caused by electric potential gradients across the electrolyte.^{90,91}

With the components of the electrolyte in mind, different combinations of salt and solvent type can be categorized into different classes. The terms used for these classes in this review are presented in Table 1. One of the earliest published electrolytes, saline solution, was a mixture of a small-molecule salt and a small-molecule solvent (water). In modern times, conventional liquid electrolytes can be non-aqueous, such as mixtures of lithium salts and high-dielectric-constant organic solvents used in lithium-ion batteries. Recent advances in lithium-ion battery design have made possible bendable batteries with less chance of solvent leakage via the addition of a, usually inert, polymer or crosslinked network that is compatible with the salt

and solvent. We term this a gel electrolyte. The polymer network imbibes the conventional liquid electrolyte rendering a soft solid that does not flow, but that is flammable and remains incompatible with lithium metal. Lithium polymer (LiPo) batteries contain such gel electrolytes, but do not contain lithium metal nor what we refer to in this review as a polymer electrolyte. A polymer electrolyte is achieved by replacing the organic solvent in a conventional liquid electrolyte by a polar polymer, such as PEO. A polysolvent, such as PEO, acts to dissociate the salt and facilitate transport, but is not itself charged. The most commonly studied polysolvent/small-molecule salt electrolytes are aliphatic polyethers as exemplified by PEO and the lithium salt LiN(SO₂CF₃)₂ (LiTFSI).^{32, 94-99} A polyelectrolyte, on the other hand, is achieved by replacing the salt in a conventional electrolyte by a charged polymer. The small-molecule solvent acts to dissociate cations from a polyanion or anions from a polycation. In other words, the anions are covalently attached to the polymer in a polyanion and free cations, such as protons or lithium, can be generated upon dissociation. Note that the small-molecule solvent can be water from the atmosphere in the case of proton-exchange-membrane fuel cells or an organic solvent in a redox flow battery. The focus of this review is the case in which both the small-molecule solvent and the small-molecule salt of conventional liquid electrolytes are replaced by polysolvent and polyanion, respectively. ^{38, 100, 101} This we term a polymer blend electrolyte. As shown schematically in Figure 6, the polysolvent acts to dissociate cations from the polyanion. In lithium metal battery applications, the charged polymer is typically a polyanion due to the need to conduct lithium cations. Polycations are largely neglected in polymer blend electrolyte literature. In addition to the polymer blend electrolyte class, there have been a growing number of reports of electrolytes in which two different polysolvents are used. These electrolytes are formed by mixing two miscible polymers that work in conjunction to dissolve a salt. In

particular, this class of electrolytes has focused on bioderived and/or biodegradable polysolvents. This is perhaps due to the growing interest in "transient batteries" for biomedical applications whereby all components are degradable and biocompatible. The following sections will describe studies of polymer blend electrolytes and bioderived binary polysolvent blend electrolytes since 2004. The focus will be on systems of interest for solid-state batteries, especially lithium batteries.

Table 1. Terms used in this review for different classes of electrolytes.

Solvent	Salt	Class		
Small-molecule liquid	Small-molecule salt	Convectional Liquid Electrolyte		
Liquid-Polysolvent Mixture	Small-molecule salt	Gel Electrolyte		
Polysolvent	Small-molecule salt	Polymer Electrolyte		
Small-molecule liquid	Polyanion/Polycation	Polyelectrolyte		
Polysolvent	Polyanion/Polycation	Polymer Blend Electrolyte		
Polymer blend	Small-molecule salt	Polysolvent Blend Electrolyte		

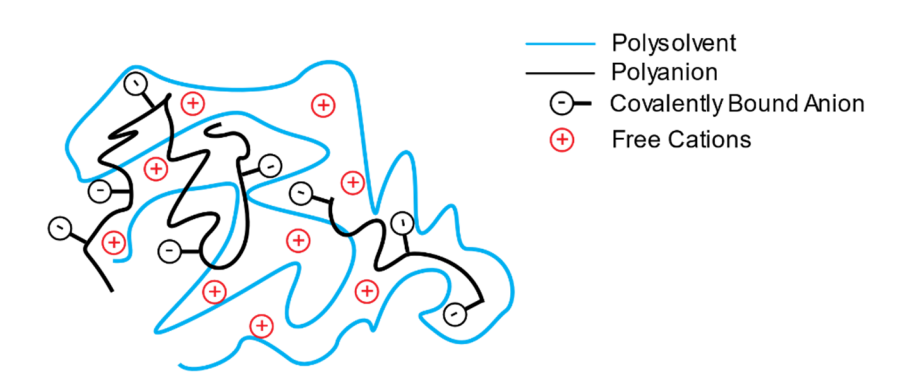


Figure 6. Schematic of a polymer blend electrolyte.

Electrolyte Performance Benchmarks

The predominant approach to characterize the potential battery performance of a new electrolyte is to measure ionic conductivity using electrochemical impedance spectroscopy (EIS).

A sinusoidal voltage (or current) is applied to a cell containing the electrolyte and the resulting complex current (or voltage) is measured over a broad range of frequency. From this data the impedance (complex resistance) is determined and used to calculate conductivity based on the geometry of the cell. The technique is quite simple to implement, straightforward to analyze, and samples are simple to prepare (electrodes need not even be reversible). For a single-ion conductor in which the anions are completely immobilized, such characterization is sufficient. However, if the anions have finite mobility, conductivity is a measure of the Ohmic resistance the will be present in an operating battery, but the picture is not complete. The term binary electrolyte will be used to refer to electrolytes in which there is one type of cation and one type of anion and both are mobile.

In terms of battery cycling rate, the limiting current density, i_L , is a useful metric. It describes the maximum achievable steady state current density, i.e. rate of charge transfer per unit electrode area. i_L is defined as the current at which the ion concentration goes to zero at one of the electrodes. It is determined by the mutual diffusion coefficient of neutral ion pairs, D, and transference number, t_+ ,

$$i_L = \frac{2DFc_{avg}}{(1 - t_+)L} \qquad (12)$$

as well as the average salt concentration, c_{avg} , and electrolyte thickness, L^{91} Equation 12 only holds in the dilute limit. To determine rate limits in concentrated electrolyte, especially those with concentration-dependent transport parameters, numerical modeling is necessary, but values of D and t_+ are still needed. Experimentally, the limiting current can be detected as the current at which the cell potential diverges to $\pm \infty$. This is due to the concentration overpotential,

$$U_{conc} = (1 - t_{+}) \frac{RT}{F} \ln \left(\frac{c_{I}}{c_{II}}\right) \quad (13)$$

diverging when the concentration at either electrode, c_I or c_{II} , goes to zero.

To fully define the transport of ions through a binary electrolyte, and thus the steady state current density, three transport parameters must be specified. In the literature, the cationic transference number (t_+) , the diffusion coefficient (D), and ionic conductivity (κ) are used to describe the transport of ions in the electrolyte. He interplay of these parameters in predicting the steady-state current density will be discussed in terms of the Newman number later, but they are presented in Table 2 for representative systems from most of the electrolyte classes defined above. As shown in Table 2, polysolvent/small-molecule salt electrolytes and polymer blend electrolytes are a promising means to increase the energy density of a battery due to their stability with respect to the energy dense lithium electrode. However, reduced values of κ and D lead to large Ohmic resistance and reduced i_L .

Table 2. Transport parameters and electrochemical stability window of representative electrolytes.

Class	Composition	T	κ	D	t_+	Stability vs Li/Li ⁺		Ref.
		(°C)	(S/cm)	(cm^2/s)		(V) Red.	Ox.	
Aqueous Liquid/ Salt Mixture	1.9 M H ₂ SO ₄ in Water	22	2×10^{-1}	2×10^{-5}	0.80	2.2	4.3	16
Organic Liquid/ Salt Mixture	1 M LiPF ₆ in EC/DMC	22	1×10^{-2}	3×10^{-6}	0.38	1.3	4.6	16, 109
Polysolvent/ Salt Mixture	1.5 M LiTFSI in PEO	85	1×10^{-3}	3×10^{-7}	0.41	0.5	3.8	16
Polymer Blend Electrolyte	63 wt% PEO 37 wt% LiPSFSI	70	5×10^{-5}	NR	0.9	0.0	4.5	38
Polysolvent Blend Electrolyte	24 wt% Dextran 36 wt% Chitosan 40 wt% LiClO ₄	25	5×10^{-3}	NR	0.98*	< 0	2.3	110, 111

 t_{+} range for studies reviewed in this class are 0.51-0.98.

A useful benchmark for polymer blend electrolytes is the PEO/LiTFSI polysolvent/small-molecule salt electrolyte. PEO/LiTFSI has long been the leading polymer electrolyte due to its high conductivity, facile processability, and chemical stability. ^{13, 16, 94, 95} Work has been done to quantify the dependence of PEO molecular weight on the transport properties of the PEO/LiTFSI system. Researchers have found that the PEO/LiTFSI system loses sensitivity to PEO molecular weight above 10 kg/mol (*N*~100). ^{13, 112} This is a because PEO chain diffusion becomes negligible with respect to ion transport facilitated by PEO segmental motion. ^{13, 30, 112} When a molecular weight of 10 kg/mol is exceeded, the PEO/LiTFSI system has reported conductivities on the order of 10⁻³ S/cm and has cationic transference numbers of 0.2 to 0.4 at 90 °C ¹⁶ with significant variation based on salt concentration. ^{13, 16, 30} A maximum conductivity occurs at an Oxygen:LiTFSI molar ratio of 16:1. ^{13, 16, 30} Furthermore, the electrochemical stability window of a PEO/LiTFSI polymer electrolyte is 0.5 to 3.8 V with reference to a Li electrode. Due to a relatively stable solid electrolyte interphase (SEI) that forms it is suitable for lithium metal applications. ¹⁶

While these benchmarks are helpful for electrolytes with low cationic transference numbers, special consideration is necessary for comparing PEO/LiTFSI to single-ion conductors. Namely, single-ion conductors generally have higher steady state current density than binary electrolytes of similar ionic conductivity.^{38, 113} Newman and Balsara proposed a dimensionless number, often termed the Newman Number, to enable the prediction and comparison of the steady state current density of electrolyte systems with variant transport parameters.¹¹³

$$Ne = \frac{2\kappa TR(1 - t_+^0)^2 T_h}{F^2 Dc}$$
 (14)

 T_h is the thermodynamic factor, and c is the salt concentration in molality [mol_{salt}/kg_{solvent}].

As shown in their derivation of *Ne*, the steady state current density of an electrolyte system is proportional to an effective conductivity.^{13, 113}

$$\kappa_{eff} = \frac{\kappa}{1 + Ne} \quad (15)$$

Thus, comparisons across electrolyte systems are most aptly made by comparing values of κ_{eff} . Electrolytes with the same value of κ_{eff} will have similar i_L and thus a similar power output assuming the same electrodes are used in each cell. However, due to the frequent omission of diffusion and thermodynamic factor measurement, direct comparison using this method is often impossible. Using the dilute solution approximation, it can be shown that $Ne = \frac{t_-}{t_+}$, 113 which means that $\kappa_{eff} = t_+ \kappa$ in this limit, because $t_+ + t_- = 1$. Lacking diffusion coefficient and thermodynamic factor values, the product $t_+ \kappa$ is an approximate means for comparing different electrolytes. In fact, Pesko et al. suggest that if a battery is polarized (by applying a constant voltage) the ratio of initial and steady state current yields a general and simple experimental means for finding $\kappa_{eff} = t_{+,SS} \kappa = \frac{i_{SS}}{i_0} \kappa$.

For the specific case of single-ion conductors, the limiting behavior of Ne can be exploited to further simplify electrolyte comparisons. As Equation 14 shows, $(1-t_+)$ dominates the Ne number with its square dependence. For single-ion conductors, where $t_+ \to 1$ and $Ne \to 0$, $\kappa_{eff} \cong \kappa$. Thus, non-unity t_+ acts to reduce κ_{eff} , and it is most important to account for this in binary electrolytes.

Due to extensive measurement by Pesko and Balsara, *Ne* values for the PEO/LiTFSI system for a variety of compositions are available as shown in Figure 7(a) below.⁴⁹ This enables direct comparisons between the effective conductivity of single-ion conductors and PEO/LiTFSI. As

shown in Figure 7(b), the maximum effective conductivity of PEO/LiTFSI is $\kappa_{eff}=2\times 10^{-4}$ S/cm at an LiTFSI mole fraction of 0.07 and at a temperature of 90 °C.^{49, 114} For an electrolyte to meet or exceed the optimal rate capability of PEO/LiTFSI (i.e. $\geq i_L$), it must have $\kappa_{eff}\geq 2\times 10^{-4}$ S/cm at 90 °C. For a perfect single-ion conductor, the benchmark is $\kappa\geq 2\times 10^{-4}$ S/cm. It is also worth noting that to utilize the full potential of lithium electrodes, a voltage stability window of at least 0.0 to 3.04 V vs the lithium electrode is required. Otherwise, chemical breakdown of the electrolyte will occur. To summarize, these benchmarks are reported in Table 3 for the two electrolyte classes to be reviewed: single-ion conducting polymer blend electrolytes and binary polysolvent blend electrolytes.

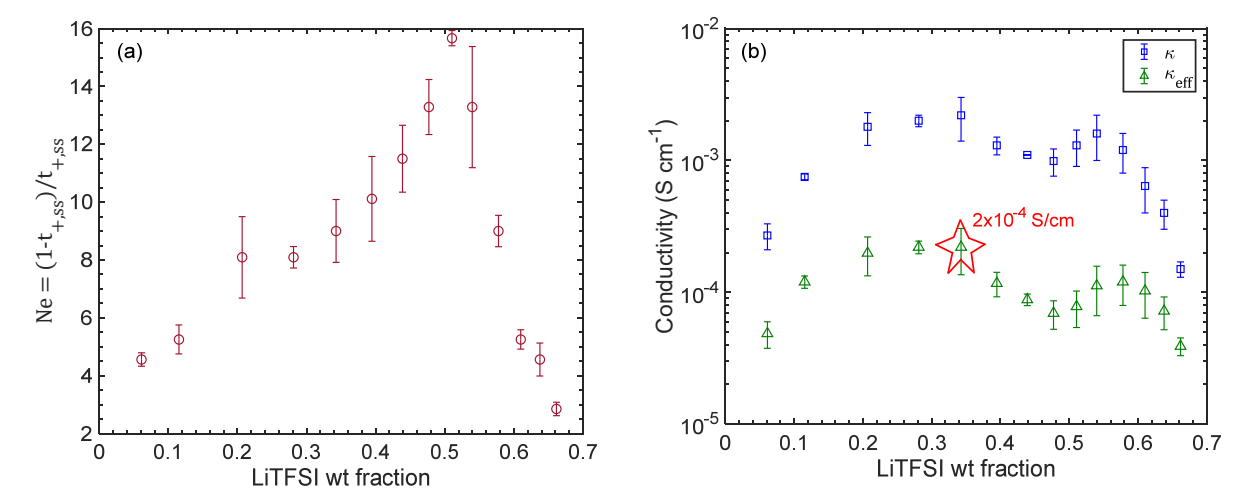


Figure 7. (a) Newman numbers and (b) conductivity and effective conductivity of PEO(5 kg/mol)/LiTFSI as a function of LiTFSI weight fraction. Values taken/calculated from Pesko et al.⁴⁹

Table 3. Performance Benchmarks of polymer blend electrolytes.

Electrolyte Type	κ_{eff}	t_{+}
	κ_{eff} (S/cm)	(unitless)
Single-Ion Conducting	10^{-4}	> 0.9
Polymer Blend Electrolytes		
Polysolvent Blend Electrolytes	10^{-3}	> 0.2

In recent reports of polymer blend electrolytes, ionic conductivity is typically measured using electrochemical impedance spectroscopy (EIS) and transference number determined using the steady state current method often termed the Bruce-Vincent Method. 19, 26, 37 Beyond transport properties, common electrolyte characterization methods include Fourier Transform Infrared (FTIR) spectroscopy, Raman spectroscopy, and nuclear magnetic resonance spectroscopy (NMR) to examine chemical interactions, ion dissociation, and diffusion. Due to widespread availability and ease for use with solid samples, FTIR has been the spectroscopic technique of choice in recent polymer blend electrolyte reports. Generally, mechanical properties and diffusion coefficients have not been reported.

Polymer Blend Electrolytes Based on Polyether Polysolvents

In recent literature, aliphatic polyether/polyelectrolyte blends are among the most studied systems. PEO is the most common polysolvent due to its high ionic conductivity of lithium ions when compared to other solid polymer electrolytes. 13, 95, 116, 117 This high ionic conductivity helps offset the lower ionic conductivity of polyanions. As described earlier, one of the largest motivations for the study of polyelectrolytes is the ability to restrict the migration of the anion without adversely impacting the mobility of the cation, thereby increasing the cation transference number. An important strategy in increasing lithium-ion mobility is the delocalization of anionic charge. Pragmatically this strategy manifests itself through large anion groups in which delocalization allows charge to be spread over a large number of atoms. Anion repeat unit structures have been included to show the growth of anion size with time. Table 4 summarizes all the polyether-based polymer blend electrolytes discussed in this section. In the Appendix,

Figure 8(a) shows the conductivity of all the studies across the entire temperature range studied, along with PEO/LiTFSI reference values. For those studies in which the transference number was reported, $\kappa_{eff}=t_+\kappa$ is shown in Figure 8(b) along with a PEO/LiTFSI reference.

Table 4. Polymer blend electrolyte performance parameters: minimum and maximum conductivity at 90 °C (unless otherwise noted), type of temperature

dependence of conductivity, and transference number at noted temperature.

Polysolvent (MW) (MW) PEO LiPSS (4000 kg/mol)		κ_{min} at 90 °C (S/cm)	κ_{max} at 90 °C (S/cm)	Temperature Dependence	(°C)	Ref.
		2×10^{-7} 77 wt% PEO	1 × 10 ⁻⁶ 69 wt% PEO	Arrhenius with slope change at T_g	0.85 (NR)	
PEO (4000 kg/mol)	LiPSFSI (M _n =9.85 kg/mol, PDI=1.40)	4.0×10^{-5} 81 wt% PEO	5.3×10^{-5} 63 wt% PEO	Arrhenius with slope change at T_g	0.9 (70)	38
PEO (4000 kg/mol)	LiPSsTFSI (M _n =200 kg/mol, PDI=2.21)	NR	1.35×10^{-4} 68 wt% PEO	Arrhenius	0.91 (60)	119
PEO (4000 kg/mol)	LiPSTFSI	NR	1×10^{-5} 77 wt% PEO	Arrhenius with slope change at T_g	0.92	120
PEO (100 kg/mol)	PLiMTFSI (50 kg/mol)	4×10^{-5} 30 wt% PEO	5×10^{-4} 50 wt% PEO	Arrhenius	NR	74
PEO (5000 kg/mol)	PA-LiTFSI	6 × 10 ⁻⁶ (80 °C) 60 wt% PEO	2 × 10 ⁻⁵ (80 °C) 50 wt% PEO	Arrhenius	0.68 (70)	121
PNE (25 kg/mol)	PNS (9 kg/mol)	1×10^{-4} 71 wt% PNE	6×10^{-3} 83 wt% PNE	Arrhenius	NR	37
PNE (25 kg/mol)	PAS (33 kg/mol)	NR	6×10^{-4} 79 wt% PNE	Arrhenius	NR	37

PEO = poly(ethylene oxide), PNE = poly(ethyleneimine)-graft-methyl(poly(ethylene glycol)), LiPSFSI = lithium poly[(4-styrenesulfonyl)(fluorosulfonyl)imide], LiPSsTFSI = poly[(4-styrenesulfonyl)(trifluorometh-yl(S-trifluoromethylsulfonyl)imide], LiPSS = lithium poly(4-styrene sulfonate), LiPSTFSI = lithium poly[(4-styrenesulfonyl) (trifluoromethanesulfonyl)imide], PA-LiTFSI = lithium poly[(trifluoromethyl) sulfonyl acrylamide], PNS = lithium 3-N-propyl sulfonate substituted poly(ethyleneimine), PAS = Lithium poly(acrylamide-2-methyl-1-propanesulfonate), PLiMTFSI = poly(lithium 1-[3-(methacryloyloxy) propylsulfonyl]-1-(trifluoromethanesulfonyl)imide), NR = not reported.

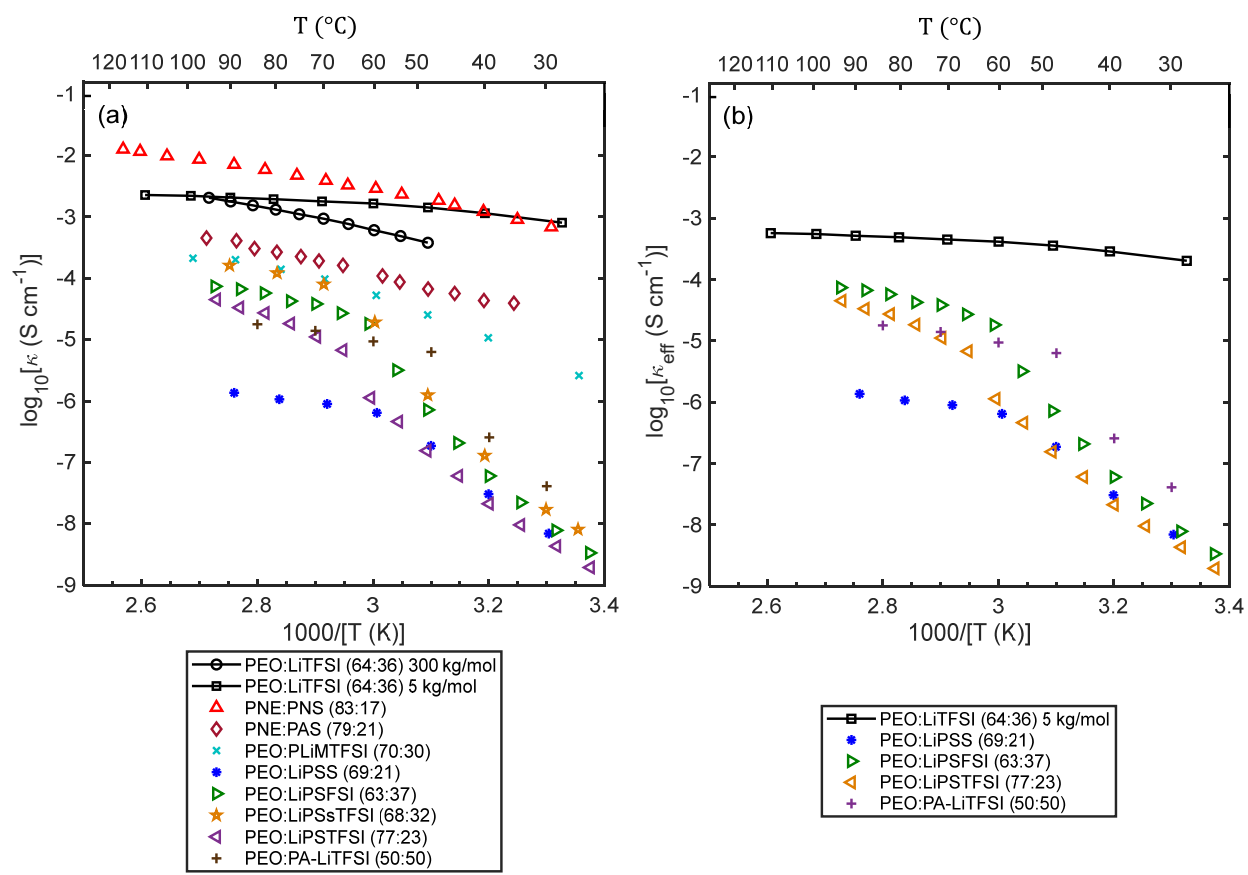


Figure 8. (a) Arrhenius plot of conductivity of polymer blend electrolytes based on polyether polysolvents along with PEO/LiTFSI reference data. (b) Effective conductivity calculated as product of conductivity and cation transference number for studies in which transference number was reported. For both figures, best performing compositions in legend are in wt%. 5 kg/mol PEO/LiTFSI data from reference ⁹⁵. 300 kg/mol PEO/LiTFSI data from reference ¹²². References for all other data are reported in Table 4.

A very early polymer blend electrolyte was lithium poly(4-styrene sulfonate) (LiPSS), shown in Figure 9. In 2004, Sun and collaborators studied LiPSS/PEO blends cast from dimethylsulfoxide. In addition to FTIR characterization, the transport properties of LiPSS/PEO blends were determined in lithium symmetric cells, but battery cycling tests were not performed. The research team found a transference number of 0.85 using the Bruce-Vincent Method and conductivities on the order of 10⁻⁵ to 10⁻⁷ S/cm at temperatures greater than 60 °C. As is common in PEO-based electrolytes, a sharp increase in conductivity was observed at 60 °C

due to melting of PEO. This early polyanion provided support for polyanion blend electrolytes due to its relatively high transference number. However, the low conductivity of this blend encapsulates the push for large anions by recent researchers. Of the anions covered in this review, sulfonate is the smallest, giving it the least delocalized charge and, therefore, strong ionic association with lithium cations. Anion-cation association reduces the concentration of free lithium ions and restricts their mobility, both of which contribute to low conductivity.

Figure 9. Lithium poly(4-styrene sulfonate) (LiPSS).

In 2016, Zhou and coworkers studied a polyelectrolyte with a larger anion: lithium poly[(4-styrenesulfonyl)(fluorosulfonyl)imide] (LiPSFSI) and its electrochemical behavior in a PEO polysolvent. ³⁸ Compared to LiPSS, LiPSFSI has an additional (fluorosulfonyl)imide group leading to more delocalization of charge, as shown in Figure 10. ³⁸ Unlike the study by Sun et al. in which LiPSS was prepared via ion exchange, Zhou et al. prepared LiPSFSI through the free radical polymerization of the functionalized monomer lithium [(4-styrenesulfonyl) (fluorosulfonyl)imide]. Blend electrolytes of PEO and LiPSFSI, cast from methanol and dried, were studied with DSC. The melting temperature of each blend occurred between 60 °C and 70 °C. Based on both DSC and X-ray diffraction (XRD) measurements, the degree of

crystallinity of PEO decreased with increasing LiPSFSI content, indicating at least partial miscibility of the two polymers. A blend with 11 mol% LiPSFSI exhibited maximum conductivity of 5.3 × 10⁻⁵ S/cm at 90 °C and an impressive Li⁺ transference number of 0.9 at 70 °C. The electrolyte was found to have a voltage stability window of 0.0 to 4.5 V versus Li/Li⁺ via cyclic voltammetry making it competitive with solid and liquid electrolytes, in this regard.^{4, 16} Thus, LiPSFSI/PEO is a promising blend as it exceeds the performance of PEO/LiTFSI in several dimensions. The mechanical properties of this blend were not reported thus making the robustness of the electrolyte unknown.

Figure 10. Lithium poly[(4-styrenesulfonyl)(fluorosulfonyl)imide] (LiPSFSI).

Lithium poly[(4-styrenesulfonyl)(trifluoromethanesulfonyl)imide] (LiPSTFSI) is a polyelectrolyte with an anion slightly larger than that of LiPSFSI. The repeat unit of LiPSTFSI is shown in Figure 11. It has seen a great deal of recent research interest, likely due to its similarity to the best performing small-molecule salt, LiTFSI. Reported glass transition temperatures for this polyanion range from 152 °C for $M_n = 68.5$ kDa to 256 °C for $M_n = 55.7$ kDa depending on processing, architecture, and molecular weight. 55, 120, 123-125 It is well known that the apparent

 T_g of polyelectrolytes is a strong function of the counter ion.⁶⁷ As such, the variability in reported T_g measurements can likely be attributed to differences in the degree of Li⁺ functionalization. LiPSTFSI has been incorporated into a number of copolymers including block polymers with PEO,^{55, 126} copolymers with methoxy-polyethylene glycol acrylate,²³ and triblock polymers with polystyrene.¹²⁷ The block polymers displayed conductivity on the order of 10^{-4} S/cm at temperatures greater than 60 °C with a high degree of single-ion conducting character.^{55, 120}

Figure 11. Lithium poly[(4-styrenesulfonyl) (trifluoromethanesulfonyl)imide] (LiPSTFSI).

When incorporated into blends, LiPSTFSI is a promising polyanion. In 2011, Armand and collaborators blended LiPSTFSI with PEO to form polymer blend electrolytes. ¹²⁰ Of note in this study was the effect of synthesis method on the performance of the electrolyte. The LiPSTFSI polyanion was generated through two routes: free radical polymerization of charged monomer and modification of commercially available sodium poly(4-styrene sulfonate) (NaPSS). ¹²⁰ The group found that free radical polymerization resulted in an approximate order of magnitude

higher conductivity when compared to the modified polymer. The authors attribute this variation to incomplete functionalization and free sulfonate groups in the modified polymer. The polymer electrolytes using the free radical polymerized polyanion had conductivity on the order of 10^{-5} S/cm. Conversely, the modified polymer had conductivities on the order of 10^{-6} to 10^{-7} S/cm. While these results make direct polymerization of the monomer seem more promising, direct modification of an existing polymer enables the retention of important polymer properties such as degree of crystallinity and molecular weight. The ease of direct modification and ability to characterize the parent polymer are additional advantages. The benefits and procedures of several common methods of generating polyanions are described in a high quality review.¹⁹

In 2013, Armand, Zhou, and coworkers continued this work by generating similar blends and block copolymers of LiPSFSI and methoxy-poly(ethylene glycol acrylate) (MPEGA).²³ Both the blends and copolymers showed extremely high thermal stability of 300 °C or higher, based on thermal gravimetic analysis (TGA).²³ With a ramp rate of 10 °C/min, TGA is a standard method to compare thermal stability among different materials, but is not indicative of long-term stability, which is less than 200 °C for PEO-containing materials even in air-free environment. With respect to conductivity, the block copolymers outperformed the homopolymer blends at low temperatures, but differences between samples were within half an order of magnitude above 60 °C. Conductivities were on the order of 10⁻⁴ S/cm⁻⁴ at 60 °C and transference numbers for each polyanion electrolyte exceeded 0.9. In the pursuit of even greater charge delocalization, Zhou, Armand and collaborators synthesized a super charge delocalized polyanion, poly[(4-styrenesulfonyl)(trifluoromethyl(S-trifluoromethylsulfonylimino)sulfonyl)imide] (PSsTFSI) in 2016.¹¹⁹ The group found an impressive ionic conductivity of 1.35 × 10⁻⁴ S/cm at 90 °C and

transference number of 0.91 at 60 °C when blended with PEO. Of note in this study was the remarkably low glass transition temperature of the neat polyanion of only 44 °C, thus enabling effective ion transport via segmental motion. These studies were key in demonstrating the viability of polymer blend electrolytes due to the similar performance of blend and copolymer electrolytes at higher temperatures.

In 2020, the trend towards larger anions was continued by Müller and colleagues. The group focused on the blending of PEO with PLiMTFSI.74 This anion has similar charge delocalization when compared to LiPSTFSI with a longer flexible sidechain between the polymer backbone and the anion, as can be seen in Figure 12. PLiMTFSI was synthesized from charged monomer achieving molecular weights from 5.5×10^3 g/mol to at least 2×10^6 g/mol. The highest molecular weight polyanion could not be characterized due to size exclusion chromatography (SEC) limitations. Due to the strength and range of electrostatic interactions, SEC of charged polymers is frequently challenging or impossible. Each polyanion was blended (via solution casting) with PEO of 100 or 1,000 kg/mol in PEO weight fractions between 0.3 and 0.95. DSC was employed to determine the miscibility of the blends from T_m depression. The group found a negative χ_{eff} ranging from -0.37 to -1.15. The values of χ_{eff} in conjunction with a single T_g indicate miscibility of the blends. Interestingly, χ_{eff} became significantly less negative with increasing PEO molecular weight. This is unlikely to be due to entropic effects because the lower molecular weight PEO was already in the high molecular weight regime (N = 730). On the other hand, χ_{eff} became more negative with increasing PLiMTFSI molecular weight (comparing blends of the two high molecular weight polyanions). Such complex behavior highlights the need for more simulations of polymer blend electrolytes.

$$\begin{array}{c|c}
CH_3 \\
 & H_2 \\
 & C \\
 & C
\end{array}$$

$$\begin{array}{c}
CH_2 \\
 & CH_2 \\
 & CH_2
\end{array}$$

$$\begin{array}{c}
CH_2 \\
 & CH_2
\end{array}$$

Figure 12. Poly(lithium 1-[3-(methacryloyloxy) propylsulfonyl]-1-(trifluoromethanesulfonyl)imide) (PLiMTFSI).

The conductivities of the PEO/PLiMTFSI blends followed complex behavior with varying levels of nonmonotonicity based on the molecular weights employed. The optimal conductivity of 5×10^{-4} S/cm at 50 wt% PLiMTFSI and 90 °C surpassed the benchmark of 2×10^{-4} S/cm, but transference numbers and battery cycling were not reported. Following the trends of χ_{eff} , conductivity was more sensitive to PEO molecular weight than that of PLiMTFSI, decreasing approximately an order of magnitude upon an increase of PEO molecular weight from 100 to 1,000 kg/mol. This shows an interesting divergence from the behavior of small molecule salts in polysolvents. Balsara's group reported minimal changes in conductivity above a polysolvent molecular weight of 10 kg/mol for PEO/LiTFSI. 30, 128 This divergence can be rationalized by the fact that polyanions can entangle with the PEO matrix, whereas small-molecule anions cannot. Müller and collaborators used dielectric spectroscopy to determine the mobility and density of ions in the PEO/PLiMTFSI electrolyte. The largest takeaway from their work was the prediction

that ion mobility is much more significant than ion density in the temperature dependence of the conductivity of PLiMTFSI.

Another study of note was completed by Piszcz and collaborators in 2016. The group synthesized a novel single-ion conductor, lithium poly[(trifluoromethyl) sulfonyl acrylamide] (PA-LiTFSI), whose repeat unit is shown in Figure 13.¹²¹ PA-LiTFSI is a functionalized version of poly(acrylic acid) (PAA) and represents a new family of polyanions for study. Blend electrolytes of PA-LiTFSI in a PEO polysolvent were constructed using solution casting with a 50:50 volume ratio of acetonitrile and methanol. The group used DSC to determine that the T_q of an equimolar blend of PEO and PA-LiTFSI was 42 °C. TGA indicated that the blend was stable up to 250 °C. The single glass transition temperature suggests miscibility, although strangely the authors report that thermal transitions were not a function of blend composition. FTIR was also employed to characterize the blend and detailed peak assignments were made. Symmetric lithium cells were used for electrochemical characterization. The group used cyclic voltammetry to determine that the stability window was 0 to 5.5 V versus Li/Li⁺, making it the most electrically stable electrolyte covered in this review. This is surprising since PEO/LiTFSI is not stable above 4 V, and this finding deserves further investigation. The Bruce-Vincent Method was used to calculate the transference number of 0.68 at 70 °C for an equal mass blend of PEO and PA-LiTFSI. EIS was used to determine that the equal mass blend had a conductivity of 2 × 10⁻⁵ S/cm at 80 °C. Of all the polymer blend electrolytes reviewed, this study was the only one that investigated battery cycling. They used a 50 wt.% blend of PEO/PA-LiTFSI as the electrolyte and binder in a LiFePO₄ cathode. At a cycling rate of C/20, the group found a decay in specific discharge capacity from a high of 140 mAh/g on the second cycle to a low of 125 mAh/g on the fifth cycle, after which the cell failed. Rapid cell failure combined with Coloumbic efficiency of less than 97% indicates that much work remains to demonstrate the feasibility of polymer blend electrolytes in functioning batteries. Despite these complications, Piszcz and collaborators' work is of particular interest due to the synthetic simplicity (one pot modification of PAA). This may make PA-LiTFSI an accessible single-ion conductor for further study despite its modest transference number and conductivity. This work further highlights the importance of battery cycling in full characterization of new electrolytes, an effort that is largely lacking in the polymer blend electrolyte literature.

$$Li^{\bigoplus}$$
 O
 NSO_2CF_3
 n

Figure 13. Lithium poly[(trifluoromethyl) sulfonyl acrylamide] (PA-LiTFSI).

In 2014, Granados-Focil and coworkers used a unique approach where the ether polysolvent moieties were grafted onto a linear main chain.³⁷ More specifically, the group synthesized and characterized single-ion conducting blends of two classes of polymers based on linear poly(ethyleneimine) (LPEI) main chains: one with a solvating side group and the other with an ion donating group. The polysolvent had sidechains constituted of 8 poly(ethylene glycol) (PEG) repeat units. The resulting polysolvent was LPEI-*graft*-methylPEG (PNE). The polyanion was LPEI with N-propylsulfonate side groups (PNS). PNE-PNS random copolymers were also synthesized for comparison. The group found that the random copolymers had conductivities several orders of magnitude lower than their blend counterparts despite having similar T_q . The group attributed this to interfacial interactions between sulfonates of the

polyanion and ether oxygens of the polysolvent. The maximum conductivity for the PNE/PNS blend occurred at an oxygen to lithium ratio of 16:1 and was 6×10^{-3} S/cm at 90 °C. In addition to surpassing the benchmark, PNE/PNS blends were compared to PNE blends with another polyanion, lithium poly(acrylamide-2-methyl-1-propanesulfonate) (PAS, 33 kg/mol). The PNE/PNS blend conductivity was more than an order of magnitude higher than PNE/PAS blends, perhaps pointing to the importance of the nitrogen in the PNS backbone; see Appendix for full table of chemical structures. Furthermore, PNE doped with LiTFSI outperforms the archetypical PEO/LiTFSI system by up to an order of magnitude. Thus, PNE is an extremely promising polysolvent both for polymer electrolytes and polymer blend electrolytes. The authors did not directly measure the transference number, but speculate it is more than 0.9. The voltage stability window of the PNE/PNS blend was reported as $\pm 5 V$ without a specific reference electrode being stated, and each blend component was found to be thermally stable up to 130 °C via TGA. This study shows the viability of amine based polysolvents and suggests a promising avenue for innovation in the field

In general, these studies suggest that polymer blend electrolytes have transference numbers significantly greater than the PEO/LiTFSI electrolyte system but with significantly reduced conductivity (at least one order of magnitude in most cases). A key persistent principle common in these systems is large charge-delocalized anions that enable the dissociation of lithium cations without causing strong association between cation and anion that would inhibit cation transport and induce an immiscibility gap in the blend phase diagram. These polyanions have significantly higher T_g than PEO, as is the case generally for polyelectrolytes due to the profound effect that electrostatic interactions have on increasing T_g . Chain connectivity of polyanions and steric impediments to chain flexibility caused by large pendant groups could contribute to reduced

conductivity. Despite the reduced absolute conductivity, examination of κ_{eff} is necessary to determine if the polymer blend electrolytes can achieve steady state current densities comparable to the PEO/LiTFSI benchmark. As shown Figure 8(b), LiPSFSI/PEO has $\kappa_{eff} = 0.9 \times 10^{-4}$ S/cm, nearly reaching the benchmark. PNS/PNE and PLiMTFSI/PEO surpass the conductivity benchmark, but do not have reported transference numbers, making them extremely promising avenues for further study. With voltage stability windows in excess of 0.0 to 4.5 V versus Li/Li⁺, some of these blends hold potential for use with high-voltage batteries (> 4 V), attractive for increased energy density.

Despite all this, a lack of focus on the mechanical properties of polymer blend electrolytes makes their robustness unclear. With the extremely reactive nature of lithium metal, it is essential that the electrolyte can withstand wear and suppress uneven SEI growth. Even in the absence of lithium metal, a solid electrolyte must function as both electrolyte and separator, preventing battery short circuit. An electrolyte that flows obviously cannot do this. Further study into the mechanical properties of promising polymer blend electrolytes is therefore recommended. Although some polymer blend electrolyte systems meet the polymer electrolyte (PEO/LiTFSI) benchmark, they still lag the conductivity of liquid electrolytes. As Table 2 shows, κ_{eff} is nearly 4×10^{-3} S/cm for organic liquid electrolyte and nearly 2×10^{-1} S/cm for aqueous electrolyte. Thus, a significant breakthrough will be required for polymer blend electrolytes to compete in the high current density domain in which contemporary liquid electrolytes dominate. To aid in these advancements, future works should report measurements of $t_{+,SS}$, diffusion coefficients, and mechanical properties of polymer blend electrolytes as this would be helpful in comparing electrolyte systems. The Newman Number acts as a potential means to relate transport parameters to steady state current density, a limiting factor in the

expansion of polymer electrolyte technologies. Similarly, shear modulus of electrolyte systems could aid in the modeling of dendrite formation, another key area that requires development.

Lastly, the construction and cycling of batteries is a rare but important method to characterize polymer electrolytes and to advocate for their real-world utilization. In any case, polymer blend electrolytes comprising single-ion conductors offer a clear use case: high energy density and high interfacial stability but at the cost of low power output.

Bioderived Polysolvent Blend/Salt Systems

Another class of electrolyte with a high degree of recent research interest is the binary polysolvent blend electrolyte composed of bioderived elements. Many of these polymers offer the unique advantage of being biodegradable and carbon neutral therefore assuaging environmental concerns with hydrocarbon-derived plastics. ¹²⁹⁻¹³¹ Chitosan, dextran, lignin, and methyl cellulose have been considered in most depth due to their respectable ionic conductivity and transference number when incorporated into binary polysolvent blend electrolytes. ^{110, 111, 132-143} The seaweed derivative, iota-carrageenan, has been used as a polysolvent in recent works without a second polysolvent and is thus worth noting despite it not being a blend. ^{144, 145} Many of these blends rely upon small-molecule solvents – particularly glycerol – to raise their conductivity above 10⁻⁶ S/cm and thus do not fit a strict definition of a polymer electrolyte. ^{132, 135}

Chitosan is of particular interest due to its rare cationic properties among polysaccharides.¹⁴⁶ If chitosan is cast in a protic environment, protons donated to the primary amine may serve to associate with anions, thus possibly explaining the high cation transference numbers reported in

Table 5.¹⁴⁷ Table A2 in the appendix shows the neutral and protonated molecular structures of chitosan, where X⁻ represents the anion of the salt used in the electrolyte. Many recent studies report chitosan cation transference numbers of greater than 0.9.^{111, 133} The use of a polycation to coordinate anions of a salt opens up an exciting approach for designing single-ion conductors without polyanions.

Recent studies into bioderived electrolyte materials have followed a similar experimental protocol as the polymer blend electrolytes where FTIR is employed for characterization, EIS is used for measuring conductivity, cyclic voltammetry is employed to measure voltage stability, and the Bruce-Vincent Method is implemented to measure the transference number.

One such study was completed in late 2020 by the Saroj research group. ¹⁴⁸ Biopolymer binary polysolvent blends were generated using poly(vinyl alcohol) (PVA) and chitosan with a sodium iodide salt (NaI). Binary polysolvent blend electrolytes were made with 10, 20, 30, 40, and 50 wt% chitosan with PVA. The thermal decomposition of each blend was studied via TGA. Specifically, the group found that the decomposition of the blend occurs in 4 stages between 193 °C and 430 °C. While not a completely monotonic relationship, increasing the mole fraction of cellulose generally decreased the thermal stability of the blend. The group used stainless steel symmetric cells to measure the ionic conductivity of each sample. At 30 °C, the 10 wt% chitosan sample displayed the highest ionic conductivity of 1.2×10^{-5} S/cm. Furthermore, the t_+ was found to be between 0.98 and 0.94 at 30 °C, making these blends remarkably effective single-ion conductors. This high degree of ion selectivity may be due to the utilization of acetic acid (a protic solvent). The high initial thermal decomposition temperature of 193 °C and near unity transference number make this system stand out as a thermally robust and near single-ion conductor

In another 2020 study that mirrored the grafted LPEI of Granados-Focil and coworkers, the Chung and Hallinan groups grafted poly(ethylene glycol) (PEG) onto a lignin main chain using a photoredox thiol-ene reaction.^{37, 149} Lignin was intended to provide mechanical strength to the copolymer while the PEG was to provide ionic conductivity and flexibility. Two different PEG molecular weights, 550 g/mol and 2000 g/mol, were used to synthesize two different PEG-graftlignin copolymers. Although not strictly polysolvent blends, the biobased graft copolymers were mixed with LiTFSI salt to form electrolytes. The conductivity was measured with EIS at a molar ratio of Li:O of 1:11.8. The biobased graft copolymer electrolyte was found to outperform PEO/LiTFSI at ambient temperatures but were less competitive above 40 °C. A conductivity of 1.4×10^{-4} S/cm at 35 °C was noted for the copolymer with 2000 g/mol PEG grafts. Thus, this copolymer is promising for room temperature applications. Direct measurement of the mechanical properties, voltage stability, and transference number of this copolymer were not reported, and thus additional research is needed to verify the compatibility with lithium metal batteries. Of note in this work are the authors attention to scalability, with special care to choose a simple three-step reaction mechanism and inexpensive reagents. Consideration of the eventual large-scale manufacture of electrolytes is typically lacking in the literature, and its inclusion in this work strengthens the prospective use of lignin-based electrolytes.

In 2020, another plant derivative, agar-agar, was utilized by Jaisankar and coworkers in a polymer blend of chitosan, PEG, and agar-agar with lithium perchlorate (LiClO₄).¹¹¹ Agar-agar is derived from seaweed and is thus a carbon neutral, biodegradable species. The chitosan used in this work was derived directly from local shells of *P. monodon*, i.e. the "giant tiger prawn". Solution casting with water and acetic acid was employed to generate the electrolyte films, once again lending some credence to the idea that cationic chitosan is formed. The group employed

the Bruce-Vincent Method to measure a transference number of 0.94 at room temperature for the most conductive blend, which had an ionic conductivity of 4.6×10^{-4} S/cm also at room temperature. FTIR was employed to examine the purity of the chitosan, indicated by major characteristic peaks such as the C-O stretching absorbance at 1024 cm^{-1} , although it is shifted from other sources. The FTIR spectrum shown in this work lacks the resolution to clearly see more subtle phenomena. Thus, careful consideration should be taken in the further pursuit of this otherwise promising system.

Other studies have focused on blends with chitosan, dextran, and cellulose derivatives. 133, ¹³⁶⁻¹³⁸ Cellulose is the most common natural polymer in the world, making up the structural components of plant life¹⁵¹ while chitosan is a derivative of exoskeletons and fungi. 111, 130 One such study was completed by the Khiar and coworkers in 2018. The research team used the ionic liquid 1-butyl-3-methylimidazolium bis(trifluoromethyl sulfonyl) imide (BMIMTFSI) in their chitosan/methyl cellulose blends. A dilute acetic acid casting solution was employed in this study. The highest observed conductivity of this system was 1.0×10^{-5} S/cm with a transference number of 0.89 at 90 °C. These trends generally hold true throughout the literature regarding this system, with ionic conductivities on the order of 10^{-5} S/cm and transference numbers exceeding 0.9 with voltage stabilities of approximately 0 to 2.5 V using stainless steel electrodes. 111, 132, 133, 140, 152, 153 A 2019 study by Aziz and collaborators studied a similar system, chitosan and dextran with similarly promising results. 110 Once again, a dilute acetic acid casting solution was used in the preparation of blends. The group found a maximum conductivity of 5.2×10^{-3} S/cm and a remarkable transference number of 0.98. Once again, the electrochemical stability window was smaller than most solid electrolytes at 0.0 to 2.3 V using stainless steel electrodes.

In addition to acting as solvents, efforts have also been made to use bioderived compounds as plasticizers. One such plasticization attempt was made with wheat flour in PEO. In 2017, Wang and collaborators created a solid polymer electrolyte consisting of PEO (4 × 10⁶ g/mol), store-bought wheat flour, and LiTFSI. The wheat flour was added to the PEO electrolyte in ratios ranging from 10:1 to 4:1 PEO to wheat flour. The group found that a PEO:wheat ratio of (9:1) led to an optimal conductivity of 2.6 × 10⁻⁵ S/cm at room temperature and a cationic transference number of 0.51. While not supported by XRD, the group argued that the linear nature of the Arrhenius conductivity plot suggests the complete disruption of PEO crystals. The group assembled a battery using a LiFePO4 cathode and an electrolyte composed of 64 wt% PEO, 7 wt% wheat, and 29 wt% LiTFSI. The group found the battery to be stable at room temperature, with a stable specific capacity of approximately 130 mAh/g for 80 cycles at 25 °C and a discharge plateau of 3.37 V. Thus, the work of Wang and coworkers is a good example of the potential efficacy of bioderived plasticizers.

A similar work carried out by Vanitha and collaborators studied the plasticizing effects of cornstarch in a poly(vinyl pyrrolidone)/ammonium chloride (PVP/NH₄Cl) polysolvent blend electrolyte. The group used solution casting to prepare symmetrical silver cells for EIS. The maximum conductivity at 85 °C of 6×10^{-6} S/cm occurred at an 80:20 cornstarch: PVP mass ratio and 25 wt% salt. The conductivity exhibited a sharp drop off at 30 wt% salt. Of note in this study is the extremely high mass percent of cornstarch in the most conductive blend. This sheds doubt on if the mechanical properties of PVP are retained by the blend, so further mechanical testing would augment the conclusions of Vanitha and collaborators. Other efforts in natural plasticizers include egg shells and starch derived from cassava. These works highlight the

possibility for nontoxic and low-cost plasticizers further reducing the environmental impacts of polymer electrolytes.

Due to the high transference number of chitosan, dextran, and methyl cellulose blend electrolytes, the possibility of natural single-ion conductors is a likely direction in the blend electrolytes field. 110, 133, 152, 153 While not mentioned by researchers, the near universal use of acetic acid as a casting solution may be key in the high cation transference of chitosan blend electrolytes, due to the formation of a chitosan polycation. This unique property of chitosan deserves further critical analysis due to its efficacy as a single ion conductor. Studies employing titration, zeta potential measurements, or even pulsed-field gradient nuclear magnetic resonance (PFG-NMR) could be valuable first steps in increasing knowledge of this plentiful bioderived electrolyte. However, the poor oxidative stability of these systems, typically less than 2.5 V, and low conductivity, typically two orders of magnitude less than PEO/LiTFSI, are serious impediments to the advancement of this technology. 110, 132, 143, 148, 153 Newman Number analysis does make several of these systems seem competitive, particularly PVA/chitosan, PVA/dextran, and agar-agar/chitosan/PEG. As shown in Figure 14, each of these systems surpasses the 10⁻⁴ S/cm single-ion conducting benchmark outlined previously, suggesting similar steady state current density to PEO/LiTFSI. Efforts to decrease the degree of crystallinity of chitosan through plasticization may increase the conductivity to more acceptable levels, but the limited oxidative stability window must be addressed for lithium battery applications to be viable. However, the extreme abundance of these materials makes them attractive for further study.

Figure 14 shows the temperature dependence of ionic conductivity for the electrolytes discussed in this section. Table 5 summarizes key results of the studies discussed in this section. The repeat unit of each structure in Table 5 is reported in the Appendix in Table A2.

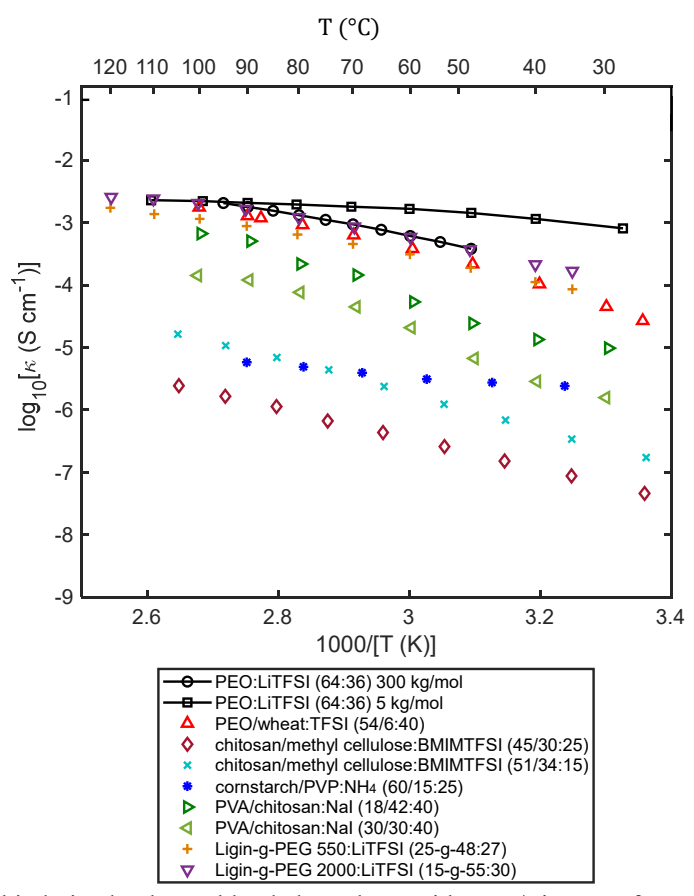


Figure 14. Conductivity of bioderived polymer blend electrolytes with PEO/LiTFSI reference. Best performing compositions in legend are in wt%. 5 kg/mol PEO/LiTFSI data from reference ⁹⁵. 300 kg/mol PEO/LiTFSI data from reference ¹²². References for all other data are reported in Table 5.

Table 5. Minimum and maximum conductivity at noted temperature (if reported) and composition, temperature dependence of conductivity, and transference numbers of bioderived polysolvent blend electrolytes.

Polysolvents	Salt	κ _{min} (S/cm)	κ _{max} (S/cm)	T Dep.	(°C)	Ref.
PEO	LiTFSI	NA	1×10^{-3}	VFT	0.51	103
Wheat Flour			(80 °C)		(25 °C)	
			64 wt% PEO			
			7 wt% Wheat			
			29 wt% LiTFSI			
Chitosan	BMIMTFSI	1.6×10^{-6}	1.0×10^{-5}	Arrhenius	0.89	133
Methyl Cellulose		(95 °C)	(95 °C)			
•		51 wt% Chitosan	45 wt% Chitosan			
		34 wt% Methyl cellulose	30 wt% Methyl cellulose			
		15 wt% BMIMTFSI	25wt% BMIMTFSI			
Chitosan	LiClO ₄	1.8×10^{-4}	4.6×10^{-4}	N/A	0.94	111
Agar Agar		(25 °C)	(25 °C)		(25 °C)	
PEO		42.5 wt% Chitosan	37.5 wt% Chitosan			
		42.5 wt% Agar Agar	37.5 wt% Agar Agar			
		5 wt% PEG	15 wt% PEG			
		10 wt% LiClO ₄	10 wt% LiClO ₄			
PVA	NaI	1.1×10^{-4}	5.0×10^{-4}	Arrhenius	0.94-0.98	148
Chitosan		30 wt % Cellulose	18 wt % Cellulose		(30 °C)	
		30 wt% PVA	42 wt% PVA			
		40 wt% NaI	40 wt% NaI			
Chitosan	LiClO ₄	5.0×10^{-10}	5.2×10^{-3}	N/A	0.98	110
Dextran		(25 °C)	(25 °C)		(25 °C)	
		40 wt.% Dextran	24 wt.% Dextran			
		60 wt.% Chitosan	36 wt.% Chitosan			
			40 wt.% LiClO ₄			
Cornstarch	NH ₄ Cl	3×10^{-7}	6×10^{-6}	Arrhenius	NR	154
PVP		(85 °C)	(85 °C)			
		19 wt.% PVP	15 wt.% PVP			
		76 wt.% Cornstarch	60 wt.% Cornstarch			
		5 wt.% NH ₄ Cl	25 wt.% NH ₄ C1			

PVA = poly(vinyl alcohol), PVP = poly(vinyl pyrrolidone), BMIMTFSI = 1-butyl-3-methylimidazolium bis(trifluoromethyl sulfonyl) imide, NR = not reported

Outlook

In recent years, research effort has been applied to enhance the viability of polymer electrolytes. While not intended as a comprehensive review of these new developments, the following section highlights some promising advances in the field of blend electrolytes to decouple the mechanical and conductivity properties of polymer electrolytes using nanoparticles. These advancements may prove key in enabling the suppression of lithium dendrites while retaining the conductivity of polymer electrolytes.

In recent literature, one promising design innovation has been the incorporation of polymer nanoparticles into polymer electrolytes to increase the mechanical strength of the polymer while simultaneously retaining or improving the conductivity of the blend. The resulting electrolytes are termed hybrid electrolytes due to the incorporation of small particles in the polysolvent. Based on historical use of nanoparticles in PEO and other studies of star polymers, this approach may viably increase ionic conductivity while retaining (or even increasing) mechanical properties. In homogeneous systems, conductivity and mechanical properties are inversely related. For example, PEO/LiTFSI conductivity decreases with increasing degree of crystallinity while the modulus increases with crystallinity. 156, 157 Ion transport occurs most readily through the amorphous region of semicrystalline polysolvents. 96, 158 Plasticizers are often employed to disrupt the crystal structure of polysolvents to capitalize on the conductivity of the amorphous region but often at the cost of mechanical properties. 135, 157, 159 A high shear modulus is of particular importance in the mechanical suppression of dendrite formation as suggested in kinetic models generated by Newman and Monroe that consider the mechanical contributions to dendrite formation. 21, 160, 161 Thus, design approaches that can both increase the conductivity and mechanical strength of polysolvents are of significant interest. Towards these ends, recent work

has attempted to decouple conductivity and mechanical strength through the incorporation of star-shaped nanoparticles into the polysolvent. $^{98, 156, 162}$ In most cases, these nanoparticles are composed of a central polymeric core with high T_g arms extending outward. These hybrid electrolytes seek to reduce the crystallinity of the polysolvent (typically PEO) while offering structural support decoupling the mechanical and conductive properties. These hybrid electrolytes have been largely successful in both increasing the modulus while retaining or improving the ionic conductivity of polymer blends.

In 2017, Glynos, Sakellariou, Anastasiadis, and coworkers incorporated poly(methyl methacrylate), PMMA, nanoparticles with many arms into PEO/LiTFSI. The nanoparticles caused remarkable improvements in both the storage modulus and conductivity of the PEO blend at a given salt concentration. The storage modulus increased by roughly an order of magnitude while the conductivity increased by two orders of magnitude when compared to comparable PEO/PMMA polysolvent blends. While this is impressive, the true value of this work is the decoupling of conductivity and the shear modulus.

Various types of nanoparticles have been investigated, include nanoscale ionic materials that leverage ionic interactions for synthesis. ¹⁶³ Nanoparticles have been added to many polymer electrolyte systems including PEO/LiTFSI. ¹⁶⁴ For instance, Park and collaborators measured the impact of a four-arm miktoarm copolymer with 3 PEO arms attached to a PS chain. The group found the addition of these arms significantly increased the storage modulus and conductivity of PEO. ¹⁶⁵ The Park group used X-ray diffraction and determined that crystallinity was significantly reduced, lending credence to the idea that the modality of decoupling is through the simultaneous plasticizing and scaffolding action of nanoparticle additives.

Work has been completed for nanoparticles with inorganic silsesquioxane cores with similarly positive results. Silsesquioxane cores are cage like structures composed of a network of stable Si-O bounds with functionalized end groups as can be seen in Figure 15. One particularly interesting strategy is the incorporation of polyanion arms to the silsesquioxane core to increase the cationic transference number. In 2017, the Balsara group incorporated LiPSTFSI arms of an average length of 7 monomer units to silsesquioxane cores. 166 Hybrid electrolytes were made by adding these particles to a polystyrene-polyethylene oxide block copolymer. The group found a maximum conductivity of 1.1×10^{-5} S/cm (r = 0.085 [Li]/[0]) for their hybrid electrolytes with a transference number of roughly 0.98 according to the Bruce-Vincent Method. 166 This conductivity is an order of magnitude below reported values for PEO/TFSI but with hugely improved cation transference. 128 The Balsara group has completed similar works for hybrid electrolytes with sulfide glass cores and perfluoropolyether arms with similar results with ionic conductivities on the order of 10^{-4} S/cm and transference numbers of 0.99 making these among the most competitive polymer electrolytes. 167 As stated previously, high transference numbers repress the formation of dendrites through the elimination of concentration gradients. 19, 161, 168, 169 Thus, the use of single-ion conducting hybrid electrolytes offers the potential to suppress dendrite formation both through mechanical and transport means.

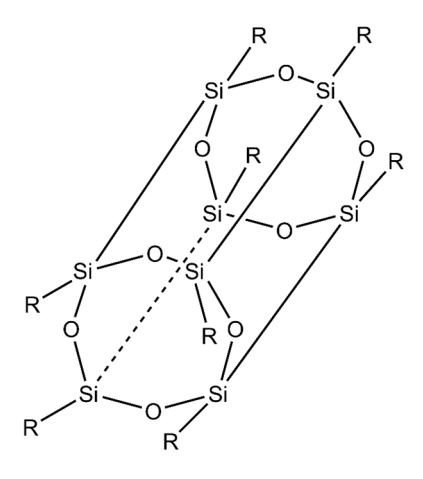


Figure 15. A polyhedral oligomeric silsesquioxane (POSS) nanoparticle core.

Another study that implemented silsesquioxane cores was completed by Saito and coworkers in 2017.¹²⁴ These researchers used a polyhedral oligomeric silsesquioxane (POSS) nanoparticle core with carboxylic acid terminated PEO arms and (4-styrenesulfonyl) (trifluromethane-sulfonyl)imide potassium anion groups attached along each arm.¹²⁴ This anion group is identical to that used in LiPSFSI, as described earlier. The group found that mixing this nanoparticle with PEO at a 20:1 O:Li ratio results in a conductivity of approximately 1.05 × 10⁻⁵ S/cm at 60 °C making it competitive with other single-ion conducting polymer electrolytes. More interestingly, the group was once again able to decouple chain dynamics and conductivity as evidenced through dielectric measurements. For a comprehensive review of the use of nanostructured polymer electrolytes, an excellent 2020 review article by Glynos and collaborators should be consulted.²¹

The use of hybrid electrolytes offers a potential means to overcome shortcomings of polymer blend electrolytes. Due to the decoupling of an electrolyte's degree of crystallinity and modulus, mechanically strong and conductive electrolytes are obtainable. Furthermore, the incorporation of polyanion arms to the nanoparticle additive gives an interesting means to tune the performance of an electrolyte. This extra degree of freedom may serve as an important parameter in electrolyte optimization. Thus, hybrid electrolytes are a promising avenue for advancement of existing polymer blend electrolyte systems.

Conclusions

The pressing need for energy dense battery technology makes recent findings in polymer blend electrolytes encouraging. The relative safety, facile production, and high specific energy of polymer blend electrolytes when compared to conventional liquid electrolyte batteries make them promising candidates for use in low current applications. However, the low ionic conductivity is a barrier to widespread adoption of this technology.

At current, the ionic conductivity of the most highly studied polymer electrolyte system, PEO/LiTFSI, still lags behind conventional liquid electrolytes by at least an order of magnitude, significantly limiting steady state current density in polymer-based batteries. Even worse, research into bioderived blend electrolytes has revealed conductivities at least several orders of magnitude less than conventional liquid electrolytes with very poor voltage stability. Single-ion conducting blend electrolytes have seen recent successes but still are unable to match the effective conductivity of PEO/LiTFSI in most cases. However, the suppression of dendrites and the inherent safety and operational benefits make single-ion conducting polymer blend electrolytes an exciting area of future research.

Promising strategies to combat these shortcomings have seen a recent focus in the literature, with hybrid electrolytes being a particularly noteworthy advancement in which nanostructure is leveraged to decouple transport and mechanical properties by providing separate mesophases,

one for ion transport and another for mechanical strength. Synergistic effects between the phases may also be present in the promising hybrid electrolytes discussed. Moving forward, work will need to address the limited steady state current densities of polymer blend electrolyte batteries to compete with the power output of conventional liquid electrolytes. Strategies for achieving this goal include designing the conductive phase to be amorphous with low T_g and/or weak coordination with lithium ions, in order to increase Li⁺ mobility ideally decoupling it from the dynamics of the polymer. In other words, materials designed to target blend miscibility via polysolvent-anion interactions should be pursued. The best performing polymer blend electrolyte and the best performing polysolvent blend electrolyte both contain nitrogen heteroatoms. Surpassing the long-standing benchmark of PEO may require a shift from predominantly oxygen heteroatoms toward nitrogen. Finally, reporting on the mechanical properties of polymer blend electrolytes, especially the shear modulus, should be an area of increased focused due to the relevance to dendrite suppression. Despite this, the ability of recent polymer blend electrolyte standouts to compete with the effective conductivity of PEO/LiTFSI is reassuring. With continued effort, the use of polymer blend electrolytes as a key component in modern energy storage seems likely.

Acknowledgments

The authors acknowledge support for this work from the National Science Foundation, award numbers 1735968, 1751450, and 1804871.

Appendix

Table A1. Repeat unit structure of polymer blend electrolytes displayed in Table 4.

Chemical Name	Abbreviation	Structure
Poly(ethylene oxide)	PEO	O
Lithium poly(4-styrene sulfonate)	LiPSS	o so o Li®
Lithium poly[(4-styrenesulfonyl)(fluorosulfonyl)imide]	LiPSFSI	0 m————————————————————————————————————
Poly[(4-styrenesulfonyl)(trifluoromethyl(S-trifluoromethylsulfonylimino)sulfonyl)imide]	LiPSsTFSI	O O O CF ₃ O CF ₃

Lithium poly[(4-styrenesulfonyl) (trifluoromethanesulfonyl)imide]	LiPSTFSI	O = S = O N⊕ Li O = S = O F = C = F F
Poly(lithium 1-[3-(methacryloyloxy) propylsulfonyl]-1-(trifluoromethanesulfonyl) imide)	PLiMTFSI	CH_{3} $- \left(\begin{array}{c} CH_{3} \\ C \longrightarrow C \end{array} \right)$ $C \longrightarrow C$ CH_{2} CH_{2} CH_{2} CH_{2} CH_{2} CH_{2} CH_{2} CH_{2} CH_{2} CH_{3} CH_{2} CH_{2} CH_{3} CH_{2} CH_{3} CH_{2} CH_{3} CH_{4} CH_{5} CH_{5} CH_{5} CH_{5}
Poly[(trifluoromethyl)sulfonyl acrylamide]	PA-LiTFSI	⊕ Li O N SO ₂ CF ₃
Linear poly(ethyleneimine)-graft- methyl(poly(ethylene glycol))	PNE	$R = \begin{cases} \\ \\ \\ \\ \\ \\ \\ \\ \\ \\ \\ \\ \\ \\ \\ \\ \\ \\$

Lithium 3-N-propyl sulfonate substituted linear poly(ethyleneimine)	PNS	SO ₃ Li [⊕]
Lithium poly(acrylamide-2-methyl-1-propanesulfonate)	PAS	HN O HN O SO3

Table A2. Repeat unit structure of biobased polymers displayed in Table 5.

Chemical Name	Abbreviation	Structure
Poly(ethylene oxide)	PEO	
Chitosan		H_2 H_2 H_2 H_3 H_4 H_5
Chitosan (Polycation)		OH H ₃ N X O n OH OH OH
Methyl cellulose		CH ₃ CH ₃ CH ₃ CH ₃ O O O O O O O O O O O O O O O O O O O

Poly(vinyl alcohol)	PVA	OH OH
Dextran		HO HO
Poly(vinyl pyrrolidone)	PVP	

References

- 1. Brédas, J.-L.; Buriak, J. M.; Caruso, F.; Choi, K.-S.; Korgel, B. A.; Palacín, M. R.; Persson, K.; Reichmanis, E.; Schüth, F.; Seshadri, R.; Ward, M. D., An Electrifying Choice for the 2019 Chemistry Nobel Prize: Goodenough, Whittingham, and Yoshino. *Chemistry of Materials* **2019**, 31, (21), 8577-8581.
- 2. Chen, Y.; Kang, Y.; Zhao, Y.; Wang, L.; Liu, J.; Li, Y.; Liang, Z.; He, X.; Li, X.; Tavajohi, N.; Li, B., A review of lithium-ion battery safety concerns: The issues, strategies, and testing standards. *Journal of Energy Chemistry* **2021**, 59, 83-99.
- 3. Liu, B.; Zhang, J.; Zhang, C.; Xu, J., Mechanical integrity of 18650 lithium-ion battery module: Packing density and packing mode. *Engineering Failure Analysis* **2018**, 91, 315-326.
- 4. Goodenough, J. B.; Kim, Y., Challenges for Rechargeable Li Batteries. *Chemistry of Materials* **2010**, 22, (3), 587-603.
- 5. Feng, X.; Ouyang, M.; Liu, X.; Lu, L.; Xia, Y.; He, X., Thermal runaway mechanism of lithium ion battery for electric vehicles: A review. *Energy Storage Materials* **2018**, 10, 246-267.
- 6. Zhang, X.; Sahraei, E.; Wang, K., Li-ion Battery Separators, Mechanical Integrity and Failure Mechanisms Leading to Soft and Hard Internal Shorts. *Scientific Reports* **2016**, 6, (1), 32578.
- 7. Christen, T.; Carlen, M. W., Theory of Ragone plots. *J. Power Sources* **2000**, 91, (2), 210-216.
- 8. Ziegler, M. S.; Trancik, J. E., Re-examining rates of lithium-ion battery technology improvement and cost decline. *Energy & Environmental Science* **2021**, 14, (4), 1635-1651.
- 9. Thackeray, M. M.; Wolverton, C.; Isaacs, E. D., Electrical energy storage for transportation—approaching the limits of, and going beyond, lithium-ion batteries. *Energy & Environmental Science* **2012**, 5, (7), 7854-7863.
- 10. Choudhury, S.; Agrawal, A.; Wei, S.; Jeng, E.; Archer, L. A., Hybrid Hairy Nanoparticle Electrolytes Stabilizing Lithium Metal Batteries. *Chem. Mater.* **2016**, 28, (7), 2147-2157.
- 11. Liu, Y. Y.; Lin, D. C.; Yuen, P. Y.; Liu, K.; Xie, J.; Dauskardt, R. H.; Cui, Y., An Artificial Solid Electrolyte Interphase with High Li-Ion Conductivity, Mechanical Strength, and Flexibility for Stable Lithium Metal Anodes. *Advanced Materials* **2017**, 29, (10), 8.
- 12. Cabana, J.; Monconduit, L.; Larcher, D.; Rosa Palacin, M., Beyond Intercalation-Based Li-Ion Batteries: The State of the Art and Challenges of Electrode Materials Reacting Through Conversion Reactions. *Adv. Mater.* **2010**, 22, (35), E170-E192.
- 13. Hallinan, D. T.; Villaluenga, I.; Balsara, N. P., Polymer and composite electrolytes. *MRS Bull.* **2018**, 43, (10), 759-767.
- 14. Fenton, D. E.; Parker, J. M.; Wright, P. V., COMPLEXES OF ALKALI-METAL IONS WITH POLY(ETHYLENE OXIDE). *Polymer* **1973**, 14, (11), 589-589.
- 15. Wright, P. V., Polymer electrolytes—the early days. *Electrochimica Acta* **1998,** 43, (10), 1137-1143.
- 16. Hallinan, D. T., Jr.; Balsara, N. P., Polymer Electrolytes. In *Annual Review of Materials Research, Vol 43*, Clarke, D. R., Ed. 2013; Vol. 43, pp 503-+.
- 17. Stolwijk, N. A.; Heddier, C.; Reschke, M.; Wiencierz, M.; Bokeloh, J.; Wilde, G., Salt-Concentration Dependence of the Glass Transition Temperature in PEO–NaI and PEO–LiTFSI Polymer Electrolytes. *Macromolecules* **2013**, 46, (21), 8580-8588.
- 18. Benrabah, D.; Sylla, S.; Alloin, F.; Sanchez, J. Y.; Armand, M., Perfluorosulfonate-polyether based single ion conductors. *Electrochimica Acta* **1995**, 40, (13), 2259-2264.

- 19. Zhang, H.; Li, C.; Piszcz, M.; Coya, E.; Rojo, T.; Rodriguez-Martinez, L. M.; Armand, M.; Zhou, Z., Single lithium-ion conducting solid polymer electrolytes: advances and perspectives. *Chem. Soc. Rev.* **2017**, 46, (3), 797-815.
- 20. Strauss, E.; Menkin, S.; Golodnitsky, D., On the way to high-conductivity single lithium-ion conductors. *Journal of Solid State Electrochemistry* **2017**, 21, (7), 1879-1905.
- 21. Glynos, E.; Pantazidis, C.; Sakellariou, G., Designing All-Polymer Nanostructured Solid Electrolytes: Advances and Prospects. *Acs Omega* **2020**, 5, (6), 2531-2540.
- 22. Meng, N.; Lian, F.; Cui, G. L., Macromolecular Design of Lithium Conductive Polymer as Electrolyte for Solid-State Lithium Batteries. *Small* **2021**, 17, (3).
- 23. Feng, S.; Shi, D.; Liu, F.; Zheng, L.; Nie, J.; Feng, W.; Huang, X.; Armand, M.; Zhou, Z., Single lithium-ion conducting polymer electrolytes based on poly[(4-styrenesulfonyl)(trifluoromethanesulfonyl)imide] anions. *Electrochim. Acta* **2013**, 93, 254-263.
- 24. Thomas, K. E.; Sloop, S. E.; Kerr, J. B.; Newman, J., Comparison of lithium-polymer cell performance with unity and nonunity transference numbers. *Journal of Power Sources* **2000**, 89, (2), 132-138.
- 25. Fuller, T. F.; Doyle, M.; Newman, J., Simulation and Optimization of the Dual Lithium Ion Insertion Cell. *Journal of The Electrochemical Society* **1994**, 141, (1), 1-10.
- 26. Bruce, P. G.; Vincent, C. A., STEADY-STATE CURRENT FLOW IN SOLID BINARY ELECTROLYTE CELLS. *J. Electroanal. Chem.* **1987**, 225, (1-2), 1-17.
- 27. Evans, J.; Vincent, C. A.; Bruce, P. G., ELECTROCHEMICAL MEASUREMENT OF TRANSFERENCE NUMBERS IN POLYMER ELECTROLYTES. *Polymer* **1987**, 28, (13), 2324-2328.
- 28. Devaux, D.; Bouchet, R.; Gle, D.; Denoyel, R., Mechanism of ion transport in PEO/LiTFSI complexes: Effect of temperature, molecular weight and end groups. *Solid State Ionics* **2012**, 227, 119-127.
- 29. Gorecki, W.; Jeannin, M.; Belorizky, E.; Roux, C.; Armand, M., PHYSICAL-PROPERTIES OF SOLID POLYMER ELECTROLYTE PEO(LITFSI) COMPLEXES. *Journal of Physics-Condensed Matter* **1995**, 7, (34), 6823-6832.
- 30. Timachova, K.; Watanabe, H.; Balsara, N. P., Effect of Molecular Weight and Salt Concentration on Ion Transport and the Transference Number in Polymer Electrolytes. *Macromolecules* **2015**, 48, (21), 7882-7888.
- 31. Ma, Y. P.; Doyle, M.; Fuller, T. F.; Doeff, M. M.; Dejonghe, L. C.; Newman, J., The Measurement of a Complete Set of Transport-Properties for a Concentrated Solid Polymer Electrolyte Solution. *J. Electrochem. Soc.* **1995**, 142, (6), 1859-1868.
- 32. Pesko, D. M.; Timachova, K.; Bhattacharya, R.; Smith, M. C.; Villaluenga, I.; Newman, J.; Balsara, N. P., Negative Transference Numbers in Poly(ethylene oxide)-Based Electrolytes. *Journal of The Electrochemical Society* **2017**, 164, (11), E3569-E3575.
- 33. Hittorf, W., On the Migration of Ions during Electrolysis. In *The Fundamental Laws of Electrolytic Conduction*, Goodwin, H. M., Ed. Harper & Brothers: New York and London, 1899; Vol. VII, pp 49-79.
- 34. Bruce, P. G.; Hardgrave, M. T.; Vincent, C. A., THE DETERMINATION OF TRANSFERENCE NUMBERS IN SOLID POLYMER ELECTROLYTES USING THE HITTORF METHOD. *Solid State Ionics* **1992**, 53, 1087-1094.
- 35. MacInnes, D. A.; Dole, M., The transference numbers of potassium chloride. New determinations by the Hittorf method and a comparison with results obtained by the moving boundary method. *Journal of the American Chemical Society* **1931**, 53, (4), 1357-1364.

- 36. Steinrück, H.-G.; Takacs, C. J.; Kim, H.-K.; Mackanic, D. G.; Holladay, B.; Cao, C.; Narayanan, S.; Dufresne, E. M.; Chushkin, Y.; Ruta, B.; Zontone, F.; Will, J.; Borodin, O.; Sinha, S. K.; Srinivasan, V.; Toney, M. F., Concentration and velocity profiles in a polymeric lithium-ion battery electrolyte. *Energy & Environmental Science* **2020**, 13, (11), 4312-4321.
- 37. Doyle, R. P.; Chen, X.; Macrae, M.; Srungavarapu, A.; Smith, L. J.; Gopinadhan, M.; Osuji, C. O.; Granados-Focil, S., Poly(ethylenimine)-Based Polymer Blends as Single-Ion Lithium Conductors. *Macromolecules* **2014**, 47, (10), 3401-3408.
- 38. Ma, Q.; Xia, Y.; Feng, W.; Nie, J.; Hu, Y.-S.; Li, H.; Huang, X.; Chen, L.; Armand, M.; Zhou, Z., Impact of the functional group in the polyanion of single lithium-ion conducting polymer electrolytes on the stability of lithium metal electrodes. *RSC Advances* **2016**, 6, (39), 32454-32461.
- 39. Lin, K.-J.; Li, K.; Maranas, J. K., Differences between polymer/salt and single ion conductor solid polymer electrolytes. *RSC Advances* **2013**, 3, (5), 1564-1571.
- 40. Brissot, C.; Rosso, M.; Chazalviel, J. N.; Lascaud, S., In Situ Concentration Cartography in the Neighborhood of Dendrites Growing in Lithium/Polymer-Electrolyte/Lithium Cells. *J. Electrochem. Soc.* **1999**, 146, (12), 4393-4400.
- 41. Brissot, C.; Rosso, M.; Chazalviel, J. N.; Lascaud, S., Dendritic growth mechanisms in lithium/polymer cells. *J. Power Sources* **1999**, 81, 925-929.
- 42. Stalin, S.; Johnson, H. E. N.; Biswal, P.; Vu, D.; Zhao, Q.; Yin, J.; Abel, B. A.; Deng, Y.; Coates, G. W.; Archer, L. A., Achieving Uniform Lithium Electrodeposition in Cross-Linked Poly(ethylene oxide) Networks: "Soft" Polymers Prevent Metal Dendrite Proliferation. *Macromolecules* **2020**, 53, (13), 5445-5454.
- 43. Li, Z.; Huang, J.; Yann Liaw, B.; Metzler, V.; Zhang, J., A review of lithium deposition in lithium-ion and lithium metal secondary batteries. *J. Power Sources* **2014**, 254, (Supplement C), 168-182.
- 44. Xu, W.; Wang, J.; Ding, F.; Chen, X.; Nasybulin, E.; Zhang, Y.; Zhang, J.-G., Lithium metal anodes for rechargeable batteries. *Energy & Environmental Science* **2014**, 7, (2), 513-537.
- 45. Hara, M.; Eisenberg, A., Miscibility enhancement via ion-dipole interactions. 1. Polystyrene ionomer/poly (alkylene oxide) systems. *Macromolecules* **1984,** 17, (7), 1335-1340.
- 46. Molnar, A.; Eisenberg, A., Miscibility of polyamide-6 with lithium or sodium sulfonated polystyrene ionomers. *Macromolecules* **1992**, 25, (21), 5774-5782.
- 47. Wang, Y. P.; Feng, H. Y.; Fu, Z. S.; Tsuchida, E.; Takeoka, S.; Ohta, T., Ion dissociation and conduction of Nafion/modified oligo(oxyethylene) composite films. *Polym. Adv. Technol.* **1991,** 2, (6), 295-299.
- 48. Jones, S. D.; Schauser, N. S.; Fredrickson, G. H.; Segalman, R. A., The Role of Polymer–Ion Interaction Strength on the Viscoelasticity and Conductivity of Solvent-Free Polymer Electrolytes. *Macromolecules* **2020**, 53, (23), 10574-10581.
- 49. Pesko, D. M.; Feng, Z.; Sawhney, S.; Newman, J.; Srinivasan, V.; Balsara, N. P., Comparing Cycling Characteristics of Symmetric Lithium-Polymer-Lithium Cells with Theoretical Predictions. *J. Electrochem. Soc.* **2018**, 165, (13), A3186-A3194.
- 50. Mullin, S. A. Morphology and Ion Transport in Block-Copolymer Electrolytes. University of California, Berkeley, Berkeley, CA, 2011.
- 51. Patel, S. N.; Javier, A. E.; Beers, K. M.; Pople, J. A.; Ho, V.; Segalman, R. A.; Balsara, N. P., Morphology and Thermodynamic Properties of a Copolymer with an Electronically Conducting Block: Poly(3-ethylhexylthiophene)-block-poly(ethylene oxide). *Nano Letters* **2012**, 12, (9), 4901-4906.

- 52. Inceoglu, S.; Rojas, A. A.; Devaux, D.; Chen, X. C.; Stone, G. M.; Balsara, N. P., Morphology–Conductivity Relationship of Single-Ion-Conducting Block Copolymer Electrolytes for Lithium Batteries. *ACS Macro Letters* **2014**, 3, (6), 510-514.
- 53. Jo, G.; Ahn, H.; Park, M. J., Simple Route for Tuning the Morphology and Conductivity of Polymer Electrolytes: One End Functional Group is Enough. *Acs Macro Letters* **2013**, 2, (11), 990-995.
- 54. Park, M. J.; Kim, S. Y., Ion transport in sulfonated polymers. *Journal of Polymer Science Part B: Polymer Physics* **2013**, 51, (7), 481-493.
- 55. Rojas, A. A.; Inceoglu, S.; Mackay, N. G.; Thelen, J. L.; Devaux, D.; Stone, G. M.; Balsara, N. P., Effect of Lithium-Ion Concentration on Morphology and Ion Transport in Single-Ion-Conducting Block Copolymer Electrolytes. *Macromolecules* **2015**, 48, (18), 6589-6595.
- 56. Web of Science: Analysis Tool.
- http://wcs.webofknowledge.com.proxy.lib.fsu.edu/RA/analyze.do?product=WOS&SID=8BqWV8FNHUJT2pBwQQr&field=TASCA_JCRCategories_JCRCategories_en&yearSort=false
- 57. Paul, D. R.; Bucknall, C. B., Introduction. In *Polymer Blends*, Paul, D. R.; Bucknall, C. B., Eds. Wiley: New York, 2000; Vol. Volume 1: Formulation.
- 58. Hiemenz, P. C.; Lodge, T. P., *Polymer Chemistry*. CRC Press: Boca Raton, FL, 2007; p 587.
- 59. Rubinstein, M.; Colby, R. H., *Polymer physics*. Oxford University Press: Oxford; New York, 2003; p 440.
- 60. Eitouni, H. B.; Balsara, N. P., Thermodynamics of Polymer Blends. In *Physical Properties of Polymers Handbook*, Second ed.; Mark, J. E., Ed. Springer: New York, 2007.
- 61. Merfeld, G. D.; Paul, D. R., Polymer-Polymer Interactions Based on Mean Field Approximations. In *Polymer Blends*, Paul, D. R.; Bucknall, C. B., Eds. Wiley: New York, 2000; Vol. Volume 1: Formulation, pp 55-92.
- 62. Zhou, N. C.; Xu, C.; Burghardt, W. R.; Composto, R. J.; Winey, K. I., Phase behavior of polystyrene and poly (styrene-ran-styrene sulfonate) blends. *Macromolecules* **2006**, 39, (6), 2373-2379.
- 63. Sing, C. E.; Olvera de la Cruz, M., Polyelectrolyte Blends and Nontrivial Behavior in Effective Flory–Huggins Parameters. *ACS Macro Letters* **2014**, 3, (8), 698-702.
- 64. Gao, Z.; Molnár, A.; Eisenberg, A., Blend compatibilization. In *Ionomers: Synthesis, structure, properties and applications*, Tant, M. R.; Mauritz, K. A.; Wilkes, G. L., Eds. Springer Netherlands: Dordrecht, 1997; pp 390-443.
- 65. Nijenhuis, A. J.; Colstee, E.; Grijpma, D. W.; Pennings, A. J., High molecular weight poly(l-lactide) and poly(ethylene oxide) blends: thermal characterization and physical properties. *Polymer* **1996**, 37, (26), 5849-5857.
- 66. Kim, K.; Kuhn, L.; Alabugin, I. V.; Hallinan, D. T., Lithium Salt Dissociation in Diblock Copolymer Electrolyte Using Fourier Transform Infrared Spectroscopy. *Frontiers in Energy Research* **2020**, 8, (240).
- 67. Kusoglu, A.; Weber, A. Z., New Insights into Perfluorinated Sulfonic-Acid Ionomers. *Chem. Rev.* **2017**, 117, (3), 987-1104.
- 68. Cristovan, F. H.; Nascimento, C. M.; Bell, M. J. V.; Laureto, E.; Duarte, J. L.; Dias, I. F. L.; Cruz, W. O.; Marletta, A., Synthesis and optical characterization of poly(styrene sulfonate) films doped with Nd(III). *Chem. Phys.* **2006**, 326, (2), 514-520.
- 69. Flory, P. J., *Principles of polymer chemistry*. Cornell University Press: Ithaca, NY, 1953; p 672.

- 70. Nishi, T.; Wang, T. T., Melting Point Depression and Kinetic Effects of Cooling on Crystallization in Poly(vinylidene fluoride)-Poly(methyl methacrylate) Mixtures. *Macromolecules* **1975**, 8, (6), 909-915.
- 71. Scott, R. L.; Magat, M., The Thermodynamics of High-Polymer Solutions: I. The Free Energy of Mixing of Solvents and Polymers of Heterogeneous Distribution. *The Journal of Chemical Physics* **1945**, 13, (5), 172-177.
- 72. Teran, A. A.; Balsara, N. P., Thermodynamics of Block Copolymers with and without Salt. *The Journal of Physical Chemistry B* **2014**, 118, (1), 4-17.
- 73. Hallinan Jr., D. T. Transport in polymer electrolyte membranes using time-resolved FTIR-ATR spectroscopy. Drexel University, Philadelphia, 2009.
- 74. Olmedo-Martínez, J. L.; Porcarelli, L.; Alegría, Á.; Mecerreyes, D.; Müller, A. J., High Lithium Conductivity of Miscible Poly(ethylene oxide)/Methacrylic Sulfonamide Anionic Polyelectrolyte Polymer Blends. *Macromolecules* **2020**, 53, (11), 4442-4453.
- 75. Alfonso, G.; Russell, T., Kinetics of crystallization in semicrystalline/amorphous polymer mixtures. *Macromolecules* **1986**, 19, (4), 1143-1152.
- 76. Runt, J. P., Crystalline Polymer Blends. In *Polymer Blends*, Paul, D. R.; Bucknall, C. B., Eds. Wiley: New York, 2000; Vol. Volume 1: Formulation, pp 167-186.
- 77. Li, X.; Hsu, S. L., An analysis of the crystallization behavior of poly(ethylene oxide)/poly(methyl methacrylate) blends by spectroscopic and calorimetric techniques. *Journal of Polymer Science: Polymer Physics Edition* **1984,** 22, (7), 1331-1342.
- 78. Lodge, T. P.; Wood, E. R.; Haley, J. C., Two calorimetric glass transitions do not necessarily indicate immiscibility: The case of PEO/PMMA. *J. Polym. Sci., Part B: Polym. Phys.* **2006**, 44, (4), 756-763.
- 79. Zhao, J. S.; Ediger, M. D.; Sun, Y.; Yu, L., Two DSC Glass Transitions in Miscible Blends of Polyisoprene/Poly(4-tert-butylstyrene). *Macromolecules* **2009**, 42, (17), 6777-6783.
- 80. Fox, T. G., Influence of Diluent and of Copolymer Composition on the Glass Temperature of a Polymer System. *Bulletin of the American Physical Society* **1956,** 1, 123.
- 81. Rieger, J., The glass transition temperature of polystyrene Results of a round robin test. *J. Therm. Anal.* **1996**, 46, (3-4), 965-972.
- 82. Rieger, J., The glass transition temperature Tg of polymers—Comparison of the values from differential thermal analysis (DTA, DSC) and dynamic mechanical measurements (torsion pendulum). *Polym. Test.* **2001**, 20, (2), 199-204.
- 83. Lunkenheimer, P.; Schneider, U.; Brand, R.; Loidl, A., Glassy dynamics. *Contemporary Physics* **2000**, 41, (1), 15-36.
- 84. Zoller, P.; Walsh, D. J., *Standard pressure-volume-temperature data for polymers*. Technomic Pub. Co.: Lancaster, PA, 1995; p 412.
- 85. Schneider, H. A., Glass transition behaviour of compatible polymer blends. *Polymer* **1989,** 30, (5), 771-779.
- 86. Alamo, R. G.; Graessley, W. W.; Krishnamoorti, R.; Lohse, D. J.; Londono, J. D.; Mandelkern, L.; Stehling, F. C.; Wignall, G. D., Small angle neutron scattering investigations of melt miscibility and phase segregation in blends of linear and branched polyethylenes as a function of the branch content. *Macromolecules* **1997**, 30, (3), 561-566.
- 87. Maurer, W. W.; Bates, F. S.; Lodge, T. P.; Almdal, K.; Mortensen, K.; Fredrickson, G. H., Can a single function for chi account for block copolymer and homopolymer blend phase behavior? *Journal of Chemical Physics* **1998**, 108, (7), 2989-3000.

- 88. Nedoma, A. J.; Robertson, M. L.; Wanakule, N. S.; Balsara, N. P., Measurements of the composition and molecular weight dependence of the Flory-Huggins interaction parameter. *Macromolecules* **2008**, 41, (15), 5773-5779.
- 89. Wignall, G. D.; Bates, F. S., APPLICATIONS AND LIMITATIONS OF DEUTERIUM LABELING METHODS TO NEUTRON-SCATTERING STUDIES OF POLYMERS. *Makromolekulare Chemie-Macromolecular Symposia* **1988**, 15, 105-122.
- 90. Bard, A. J.; Faulkner, L. R., *Electrochemical methods : fundamentals and applications*. 2nd ed.; Wiley: New York, 2001; p xxi, 833 p.
- 91. Newman, J. S.; Thomas-Alyea, K. E., *Electrochemical systems*. 3rd ed.; J. Wiley: Hoboken, N.J., 2004; p xx, 647 p.
- 92. Volta, A., On the electricity excited by the mere contact of conducting substances of different kinds. In a letter from Mr. Alexander Volta, F. R. S. Professor of Natural Philosophy in the University of Pavia, to the Rt. Hon. Sir Joseph Banks, Bart. K. B. P. R. S. Abstracts of the Papers Printed in the Philosophical Transactions of the Royal Society of London 1832, 1, 27-29.
- 93. Xu, K., Nonaqueous liquid electrolytes for lithium-based rechargeable batteries. *Chemical Reviews* **2004**, 104, (10), 4303-4417.
- 94. Edman, L.; Doeff, M. M.; Ferry, A.; Kerr, J.; De Jonghe, L. C., Transport Properties of the Solid Polymer Electrolyte System P(EO)nLiTFSI. *The Journal of Physical Chemistry B* **2000**, 104, (15), 3476-3480.
- 95. Pesko, D. M.; Webb, M. A.; Jung, Y.; Zheng, Q.; Miller, T. F.; Coates, G. W.; Balsara, N. P., Universal Relationship between Conductivity and Solvation-Site Connectivity in Ether-Based Polymer Electrolytes. *Macromolecules* **2016**, 49, (14), 5244-5255.
- 96. Borodin, O.; Smith, G. D., Mechanism of Ion Transport in Amorphous Poly(ethylene oxide)/LiTFSI from Molecular Dynamics Simulations. *Macromolecules* **2006**, 39, (4), 1620-1629.
- 97. Xu, L.; Li, J.; Deng, W.; Li, L.; Zou, G.; Hou, H.; Huang, L.; Ji, X., Boosting the ionic conductivity of PEO electrolytes by waste eggshell-derived fillers for high-performance solid lithium/sodium batteries. *Materials Chemistry Frontiers* **2021**, 5, (3), 1315-1323.
- 98. Glynos, E.; Petropoulou, P.; Mygiakis, E.; Nega, A. D.; Pan, W. Y.; Papoutsakis, L.; Giannelis, E. P.; Sakellariou, G.; Anastasiadis, S. H., Leveraging Molecular Architecture To Design New, All-Polymer Solid Electrolytes with Simultaneous Enhancement in Modulus and Ionic Conductivity. *Macromolecules* **2018**, 51, (7), 2542-2550.
- 99. Hashim, N.; Subban, R., Studies on conductivity, structural and thermal properties of *PEO-LiTFSI polymer electrolytes doped with EMImTFSI ionic liquid*. 2018; Vol. 2031, p 020021.
- 100. Rumyantsev, A. M.; de Pablo, J. J., Microphase Separation in Polyelectrolyte Blends: Weak Segregation Theory and Relation to Nuclear "Pasta". *Macromolecules* **2020**, 53, (4), 1281-1292.
- 101. Venugopalan, G.; Chang, K.; Nijoka, J.; Livingston, S.; Geise, G. M.; Arges, C. G., Stable and Highly Conductive Polycation–Polybenzimidazole Membrane Blends for Intermediate Temperature Polymer Electrolyte Membrane Fuel Cells. *ACS Applied Energy Materials* **2020**, 3, (1), 573-585.
- 102. Mittal, N.; Ojanguren, A.; Niederberger, M.; Lizundia, E., Degradation Behavior, Biocompatibility, Electrochemical Performance, and Circularity Potential of Transient Batteries. *Advanced Science* **2021**, 8, (12).

- 103. Lin, Y.; Cheng, Y.; Li, J.; Miller, J. D.; Liu, J.; Wang, X. M., Biocompatible and biodegradable solid polymer electrolytes for high voltage and high temperature lithium batteries. *Rsc Advances* **2017**, 7, (40), 24856-24863.
- 104. Zugmann, S.; Fleischmann, M.; Amereller, M.; Gschwind, R. M.; Wiemhofer, H. D.; Gores, H. J., Measurement of transference numbers for lithium ion electrolytes via four different methods, a comparative study. *Electrochim. Acta* **2011**, 56, (11), 3926-3933.
- 105. Cameron, G. G.; Harvie, J. L.; Ingram, M. D., THE STEADY-STATE CURRENT AND TRANSFERENCE NUMBER MEASUREMENTS IN POLYMER ELECTROLYTES. *Solid State Ionics* **1989**, 34, (1-2), 65-68.
- 106. Hafezi, H.; Newman, J., Verification and analysis of transference number measurements by the galvanostatic polarization method. *J. Electrochem. Soc.* **2000**, 147, (8), 3036-3042.
- 107. Newman, J.; Chapman, T. W., Restricted diffusion in binary solutions. *AlChE J.* **1973**, 19, (2), 343-348.
- 108. Mullin, S. A.; Stone, G. M.; Panday, A.; Balsara, N. P., Salt Diffusion Coefficients in Block Copolymer Electrolytes. *J. Electrochem. Soc.* **2011**, 158, (6), A619-A627.
- 109. Hallinan, D. T.; Mullin, S. A.; Stone, G. M.; Balsara, N. P., Lithium Metal Stability in Batteries with Block Copolymer Electrolytes. *J. Electrochem. Soc.* **2013**, 160, (3), A464-A470.
- 110. Aziz, S. B.; Hamsan, M. H.; Kadir, M. F. Z.; Karim, W. O.; Abdullah, R. M., Development of Polymer Blend Electrolyte Membranes Based on Chitosan: Dextran with High Ion Transport Properties for EDLC Application. *International Journal of Molecular Sciences* **2019**, 20, (13).
- 111. Edward, M. L.; Dharanibalaji, K. C.; Kumar, K. T.; Chandrabose, A. R. S.; Shanmugharaj, A. M.; Jaisankar, V., Preparation and characterisation of chitosan extracted from shrimp shell (Penaeus monodon) and chitosan-based blended solid polymer electrolyte for lithium-ion batteries. *Polymer Bulletin* **2021**.
- 112. Teran, A. A.; Tang, M. H.; Mullin, S. A.; Balsara, N. P., Effect of molecular weight on conductivity of polymer electrolytes. *Solid State Ionics* **2011**, 203, (1), 18-21.
- 113. Balsara, N. P.; Newman, J., Relationship between Steady-State Current in Symmetric Cells and Transference Number of Electrolytes Comprising Univalent and Multivalent Ions. *Journal of The Electrochemical Society* **2015**, 162, (14), A2720-A2722.
- 114. Gribble, D. A.; Frenck, L.; Shah, D. B.; Maslyn, J. A.; Loo, W. S.; Mongcopa, K. I. S.; Pesko, D. M.; Balsara, N. P., Comparing Experimental Measurements of Limiting Current in Polymer Electrolytes with Theoretical Predictions. *Journal of The Electrochemical Society* **2019**, 166, (14), A3228-A3234.
- 115. Milazzo, G.; Caroli, S.; Braun, R. D., Tables of Standard Electrode Potentials. *Journal of The Electrochemical Society* **1978**, 125, (6), 261C-261C.
- 116. Hallinan, D. T.; Balsara, N. P., Polymer Electrolytes. *Annual Review of Materials Research* **2013**, 43, (1), 503-525.
- 117. Kim, K.; Hallinan, D. T., Lithium Salt Diffusion in Diblock Copolymer Electrolyte Using Fourier Transform Infrared Spectroscopy. *The Journal of Physical Chemistry B* **2020**, 124, (10), 2040-2047.
- 118. Park, C. H.; Sun, Y.-K.; Kim, D.-W., Blended polymer electrolytes based on poly(lithium 4-styrene sulfonate) for the rechargeable lithium polymer batteries. *Electrochimica Acta* **2004**, 50, (2), 375-378.
- 119. Ma, Q.; Zhang, H.; Zhou, C.; Zheng, L.; Cheng, P.; Nie, J.; Feng, W.; Hu, Y.-S.; Li, H.; Huang, X.; Chen, L.; Armand, M.; Zhou, Z., Single Lithium-Ion Conducting Polymer

- Electrolytes Based on a Super-Delocalized Polyanion. *Angewandte Chemie International Edition* **2016**, 55, (7), 2521-2525.
- 120. Meziane, R.; Bonnet, J.-P.; Courty, M.; Djellab, K.; Armand, M., Single-ion polymer electrolytes based on a delocalized polyanion for lithium batteries. *Electrochim. Acta* **2011**, 57, 14-19.
- 121. Piszcz, M.; Garcia-Calvo, O.; Oteo, U.; del Amo, J. M. L.; Li, C. M.; Rodriguez-Martinez, L. M.; Ben Youcef, H.; Lago, N.; Thielen, J.; Armand, M., New Single Ion Conducting Blend Based on PEO and PA-LiTFSI. *Electrochimica Acta* **2017**, 255, 48-54.
- 122. Lascaud, S.; Perrier, M.; Vallee, A.; Besner, S.; Prud'homme, J.; Armand, M., Phase Diagrams and Conductivity Behavior of Poly(ethylene oxide)-Molten Salt Rubbery Electrolytes. *Macromolecules* **1994**, 27, (25), 7469-7477.
- 123. Bocharova, V.; Wojnarowska, Z.; Cao, P.-F.; Fu, Y.; Kumar, R.; Li, B.; Novikov, V. N.; Zhao, S.; Kisliuk, A.; Saito, T.; Mays, J. W.; Sumpter, B. G.; Sokolov, A. P., Influence of Chain Rigidity and Dielectric Constant on the Glass Transition Temperature in Polymerized Ionic Liquids. *The Journal of Physical Chemistry B* **2017**, 121, (51), 11511-11519.
- 124. Cao, P.-F.; Wojnarowska, Z.; Hong, T.; Carroll, B.; Li, B.; Feng, H.; Parsons, L.; Wang, W.; Lokitz, B. S.; Cheng, S.; Bocharova, V.; Sokolov, A. P.; Saito, T., A star-shaped single lithium-ion conducting copolymer by grafting a POSS nanoparticle. *Polymer* **2017**, 124, 117-127.
- 125. Liu, J.; Pickett, P. D.; Park, B.; Upadhyay, S. P.; Orski, S. V.; Schaefer, J. L., Non-solvating, side-chain polymer electrolytes as lithium single-ion conductors: synthesis and ion transport characterization. *Polymer Chemistry* **2020**, 11, (2), 461-471.
- 126. Bouchet, R.; Maria, S.; Meziane, R.; Aboulaich, A.; Lienafa, L.; Bonnet, J.-P.; Phan, T. N. T.; Bertin, D.; Gigmes, D.; Devaux, D.; Denoyel, R.; Armand, M., Single-ion BAB triblock copolymers as highly efficient electrolytes for lithium-metal batteries. *Nature Materials* **2013**, 12, (5), 452-457.
- 127. Jangu, C.; Savage, A. M.; Zhang, Z.; Schultz, A. R.; Madsen, L. A.; Beyer, F. L.; Long, T. E., Sulfonimide-Containing Triblock Copolymers for Improved Conductivity and Mechanical Performance. *Macromolecules* **2015**, 48, (13), 4520-4528.
- 128. Panday, A.; Mullin, S.; Gomez, E. D.; Wanakule, N.; Chen, V. L.; Hexemer, A.; Pople, J.; Balsara, N. P., Effect of Molecular Weight and Salt Concentration on Conductivity of Block Copolymer Electrolytes. *Macromolecules* **2009**, 42, (13), 4632-4637.
- 129. Matica, A.; Menghiu, G., Biodegradability of chitosan based products. 2017.
- 130. Angelo, L. M.; França, D.; Faez, R., Biodegradation and viability of chitosan-based microencapsulated fertilizers. *Carbohydrate Polymers* **2021**, 257, 117635.
- 131. Béguin, P.; Aubert, J. P., The biological degradation of cellulose. *FEMS microbiology reviews* **1994**, 13, (1), 25-58.
- 132. Aziz, S. B.; Hamsan, M. H.; Brza, M. A.; Kadir, M. F. Z.; Muzakir, S. K.; Abdulwahid, R. T., Effect of glycerol on EDLC characteristics of chitosan:methylcellulose polymer blend electrolytes. *Journal of Materials Research and Technology* **2020**, 9, (4), 8355-8366.
- 133. Misenan, M. S. M.; Isa, M. I. N.; Khiar, A. S. A., Electrical and structural studies of polymer electrolyte based on chitosan/methyl cellulose blend doped with BMIMTFSI. *Materials Research Express* **2018**, 5, (5).
- 134. Zhou, T. C.; He, X. M.; Lu, Z. Q., Studies on a novel anion-exchange membrane based on chitosan and ionized organic compounds with multiwalled carbon nanotubes for alkaline fuel cells. *Journal of Applied Polymer Science* **2018**, 135, (22).

- 135. Asnawi, A.; Aziz, S. B.; Brevik, I.; Brza, M. A.; Yusof, Y. M.; Alshehri, S. M.; Ahamad, T.; Kadir, M. F. Z., The Study of Plasticized Sodium Ion Conducting Polymer Blend Electrolyte Membranes Based on Chitosan/Dextran Biopolymers: Ion Transport, Structural, Morphological and Potential Stability. *Polymers* **2021**, 13, (3).
- 136. Badry, R.; El-Khodary, S.; Elhaes, H.; Nada, N.; Ibrahim, M., Optical, conductivity and dielectric properties of plasticized solid polymer electrolytes based on blends of sodium carboxymethyl cellulose and polyethylene oxide. *Optical and Quantum Electronics* **2021**, 53, (1).
- 137. Ma, X. D.; Zuo, X. X.; Wu, J. H.; Deng, X.; Xiao, X.; Liu, J. S.; Nan, J. M., Polyethylene-supported ultra-thin polyvinylidene fluoride/hydroxyethyl cellulose blended polymer electrolyte for 5 V high voltage lithium ion batteries. *Journal of Materials Chemistry A* **2018**, 6, (4), 1496-1503.
- 138. Zuo, X.; Ma, X. X.; Wu, J. H.; Deng, X.; Xiao, X.; Liu, J. S.; Nan, J. M., Self-supporting ethyl cellulose/poly(vinylidene fluoride) blended gel polymer electrolyte for 5 V high-voltage lithium-ion batteries. *Electrochimica Acta* **2018**, 271, 582-590.
- 139. Abutalib, M. M.; Rajeh, A., Structural, thermal, optical and conductivity studies of Co/ZnO nanoparticles doped CMC polymer for solid state battery applications. *Polymer Testing* **2020**, 91.
- 140. Al-Salman, Y., Conductivity and Electrical Properties of Chitosan Methylcellulose Blend Biopolymer Electrolyte Incorporated with Lithium Tetrafluoroborate. *International Journal of Electrochemical Science* **2018**, 13, 3185-3199.
- 141. Mazuki, N. F.; Abdul Majeed, A. P. P.; Nagao, Y.; Samsudin, A. S., Studies on ionics conduction properties of modification CMC-PVA based polymer blend electrolytes via impedance approach. *Polymer Testing* **2020**, 81, 106234.
- 142. Saadiah, M. A.; Samsudin, A. S., Electrical study on Carboxymethyl Cellulose-Polyvinyl alcohol based bio-polymer blend electrolytes. *IOP Conference Series: Materials Science and Engineering* **2018**, 342, 012045.
- 143. Abdulwahid, R. T.; Aziz, S. B.; Brza, M. A.; Kadir, M. F. Z.; Karim, W. O.; Hamsan, H. M.; Asnawi, A. S. F. M.; Abdullah, R. M.; Nofal, M. M.; Dannoun, E. M. A., Electrochemical performance of polymer blend electrolytes based on chitosan: dextran: impedance, dielectric properties, and energy storage study. *Journal of Materials Science: Materials in Electronics* **2021**.
- 144. Moniha, V.; Alagar, M.; Selvasekarapandian, S.; Sundaresan, B.; Hemalatha, R.; Boopathi, G., Synthesis and characterization of bio-polymer electrolyte based on iota-carrageenan with ammonium thiocyanate and its applications. *Journal of Solid State Electrochemistry* **2018**, 22, (10), 3209-3223.
- 145. Chitra, R.; Sathya, P.; Selvasekarapandian, S.; Meyvel, S., Synthesis and characterization of iota-carrageenan biopolymer electrolyte with lithium perchlorate and succinonitrile (plasticizer). *Polymer Bulletin* **2020**, 77, (3), 1555-1579.
- 146. Cheung, R. C. F.; Ng, T. B.; Wong, J. H.; Chan, W. Y., Chitosan: An Update on Potential Biomedical and Pharmaceutical Applications. *Marine drugs* **2015**, 13, (8), 5156-5186.
- 147. Chopra, H.; Ruhi, G., Eco friendly chitosan: An efficient material for water purification. *The Pharma Innovation Journal* **2016**, 5, 92-95.
- 148. Bharati, D. C.; Rawat, P.; Saroj, A. L., Structural, thermal, and ion dynamics studies of PVA-CS-NaI-based biopolymer electrolyte films. *Journal of Solid State Electrochemistry* **2021**.

- 149. Liu, H. L.; Mulderrig, L.; Hallinan, D.; Chung, H. Y., Lignin-Based Solid Polymer Electrolytes: Lignin-Graft-Poly(ethylene glycol). *Macromolecular Rapid Communications* **2021**, 42, (3), 6.
- 150. Varma, R.; Vasudevan, S., Extraction, Characterization, and Antimicrobial Activity of Chitosan from Horse Mussel Modiolus modiolus. *ACS Omega* **2020**, 5, (32), 20224-20230.
- 151. Klemm, D.; Heublein, B.; Fink, H.-P.; Bohn, A., Cellulose: Fascinating Biopolymer and Sustainable Raw Material. *Angewandte Chemie International Edition* **2005**, 44, (22), 3358-3393.
- 152. Aziz, S. B.; Hamsan, M.; Abdullah, R. M.; Abdulwahid, R. T.; Brza, M.; Marif, A. S.; Kadir, M., Protonic EDLC cell based on chitosan (CS): Methylcellulose (MC) solid polymer blend electrolytes. *Ionics* **2020**, 1-12.
- 153. Aziz, S. B.; Asnawi, A. S. F. M.; Kadir, M. F. Z.; Alshehri, S. M.; Ahamad, T.; Yusof, Y. M.; Hadi, J. M., Structural, Electrical and Electrochemical Properties of Glycerolized Biopolymers Based on Chitosan (CS): Methylcellulose (MC) for Energy Storage Application. *Polymers* **2021**, 13, (8), 1183.
- 154. Jothi, M. A.; Vanitha, D.; Bahadur, S. A.; Nallamuthu, N., Investigations of biodegradable polymer blend electrolytes based on Cornstarch: PVP: NH4Cl and its potential application in solid-state batteries. *Journal of Materials Science-Materials in Electronics* **2021**, 32, (5), 5427-5441.
- 155. Pereira, A. G. B.; Gouveia, R. F.; de Carvalho, G. M.; Rubira, A. F.; Muniz, E. C., Polymer blends based on PEO and starch: Miscibility and spherulite growth rate evaluated through DSC and optical microscopy. *Materials Science and Engineering: C* **2009**, 29, (2), 499-504.
- 156. He, D.; Cho, S. Y.; Kim, D. W.; Lee, C.; Kang, Y., Enhanced Ionic Conductivity of Semi-IPN Solid Polymer Electrolytes Based on Star-Shaped
- Oligo(ethyleneoxy)cyclotriphosphazenes. *Macromolecules* 2012, 45, (19), 7931-7938.
- 157. Menyhard, A., Direct correlation between modulus and the crystalline structure in isotactic polypropylene. *Express Polymer Letters* **2015**, 9, 308-320.
- 158. Golodnitsky, D.; Ardel, G.; Peled, E., Ion-transport phenomena in concentrated PEO-based composite polymer electrolytes. *Solid State Ionics* **2002**, 147, (1), 141-155.
- 159. Wypych, G., Handbook of plasticizers: Third edition. 2017; p 1-858.
- 160. Monroe, C.; Newman, J., The Impact of Elastic Deformation on Deposition Kinetics at Lithium/Polymer Interfaces. *Journal of The Electrochemical Society* **2005**, 152, A396-A404.
- 161. Monroe, C.; Newman, J., The Effect of Interfacial Deformation on Electrodeposition Kinetics. *Journal of The Electrochemical Society* **2004**, 151, (6), A880.
- 162. Glynos, E.; Papoutsakis, L.; Pan, W.; Giannelis, E. P.; Nega, A. D.; Mygiakis, E.; Sakellariou, G.; Anastasiadis, S. H., Nanostructured Polymer Particles as Additives for High Conductivity, High Modulus Solid Polymer Electrolytes. *Macromolecules* **2017**, 50, (12), 4699-4706.
- 163. Fernandes, N. J.; Wallin, T. J.; Vaia, R. A.; Koerner, H.; Giannelis, E. P., Nanoscale Ionic Materials. *Chem. Mater.* **2014**, 26, (1), 84-96.
- 164. Li, M.; Wang, C.; Chen, Z.; Xu, K.; Lu, J., New Concepts in Electrolytes. *Chemical Reviews* **2020**, 120, (14), 6783-6819.
- 165. Lee, D.; Jung, H. Y.; Park, M. J., Solid-State Polymer Electrolytes Based on AB3-Type Miktoarm Star Copolymers. *ACS Macro Letters* **2018**, 7, (8), 1046-1050.

- 166. Villaluenga, I.; Inceoglu, S.; Jiang, X.; Chen, X. C.; Chintapalli, M.; Wang, D. R.; Devaux, D.; Balsara, N. P., Nanostructured Single-Ion-Conducting Hybrid Electrolytes Based on Salty Nanoparticles and Block Copolymers. *Macromolecules* **2017**, 50, (5), 1998-2005.
- 167. Villaluenga, I.; Wujcik, K. H.; Tong, W.; Devaux, D.; Wong, D. H. C.; DeSimone, J. M.; Balsara, N. P., Compliant glass—polymer hybrid single ion-conducting electrolytes for lithium batteries. *Proceedings of the National Academy of Sciences* **2016**, 113, (1), 52.
- 168. Chen, Y. Z.; Li, Z.; Liu, X. P.; Zeng, D. L.; Zhang, Y. F.; Sun, Y. B.; Ke, H. Z.; Cheng, H. S., Construction of interconnected micropores in poly(arylene ether) based single ion conducting blend polymer membranes via vapor-induced phase separation. *Journal of Membrane Science* **2017**, 544, 47-57.
- 169. Berliner, M. D.; McGill, B. C.; Majeed, M.; Hallinan, D. T., Electrochemical Kinetics of Lithium Plating and Stripping in Solid Polymer Electrolytes: Pulsed Voltammetry. *Journal of The Electrochemical Society* **2019**, 166, (2), A297-A304.



Michael Blatt is a PhD candidate in the Department of Chemical & Biomedical Engineering at the FAMU-FSU College of Engineering. He has a BS degree in Chemical Engineering from SUNY Buffalo where he completed a number of industrial and academic projects in the energy and medical fields. Above all else, Michael is dedicated to education and engineering advocacy. He is active in teaching and mentoring undergraduate students, engaged in STEM outreach, and serves as the Vice President of the Polymer Chemistry / Polymeric Materials Science and Engineering (Poly/PMSE) student chapter at FSU and FAMU organizing a new annual research symposium.



Daniel T. Hallinan Jr. is an Associate Professor at the Florida A&M University—Florida State University College of Engineering with interest in fundamental polymer physics of nanostructured materials such as block copolymers and polymer-grafted nanoparticles as well as applications related to energy sustainability and artificial muscles. He is a chemical engineer with bachelors degrees from Lafayette College and a PhD from Drexel University. His post-doctoral research was conducted at Lawrence Berkeley National Lab and the University of California, Berkeley. He is involved in the polymer communities of the American Physical Society and the American Institute of Chemical Engineers. He has received an NSF CAREER Award and has testified before a U.S. Congressional Subcommittee in support of national synchrotron facilities, which his group uses extensively.